國立交通大學

資訊科學與工程研究所

碩 士 論 文

磁 振 造 影 腦 模 板 之 客 製 化 建 構

Construction of Customized Brain Template from Magnetic Resonance Images

研 究 生：李國維

指導教授：陳永昇　博士

中 華 民 國　一百 年 八 月

磁振造影腦模板之客製化建構
Construction of Customized Brain Template from Magnetic Resonance Images

研 究 生：李國維　　Student：Kuo-Wei Lee

指導教授：陳永昇　　Advisor：Yong-Sheng Chen

國 立 交 通 大 學

資 訊 科 學 與 工 程 研 究 所

碩 士 論 文

A Thesis

Submitted to Institute of Computer Science and Engineering

College of Computer Science

National Chiao Tung University

in partial Fulfillment of the Requirements

for the Degree of

Master

in

Computer Science

August 2011

Hsinchu, Taiwan, Republic of China

中華民國一百年八月

摘要

腦部的磁振造影技術（MRI），已被廣泛的使用在研究人類的腦部結構上，腦模板（template）提供一個共同對位（registration）的標準空間，做為分析腦部結構和比較腦部結構差異的基準。然而，對於一個不適當的腦模板空間，可能會造成受測者的磁振造影影像需要過大的空間形變，才能對位到腦模板上，對位後的成像容易會產生較大的誤差，對於研究分析特定族群的腦部結構，如何建構一個無偏頗（unbiased）的腦模板是必要的。

此研究的主要目的是發展一個標準的建構客製化腦模板（customized brain template）流程。首先，我們會運用影像分析，將所有的受測者影像，截取出純腦（brain-only）結構影像和不同腦組織（tissue）影像。接著，我們會選取一個參考影像當作起始的腦模板空間，藉由腦模板和受測者影像之間反覆性的影像對位流程，逐步的優化該選取的起始腦模板影像，並得到一個代表性的影像（representative image）。最後，將所有的受測者影像對位到此代表性影像亦為腦模板空間，在平均所有對位到該空間的影像後即可得到腦模板影像。

在此研究中，我們利用 216 個正常受測者（normal subject）的影像，在台灣建立一組腦模板稱為 BTT216。在和 ICBM152 腦模板的評比中，這 216 個受測者影像對位到不同的腦模板後的成像，BTT216 提供較高的影像相關性（correlation）。在平均形變量（magnitude of deformation）的評比上，BTT216 亦提供較小的形變差異。除此之外，我們針對特定的研究族群（study-specific）建立該族群的腦模板，例如不同性別和年齡層的腦模板，在評比中亦顯示此特定的腦模板影像相較於其他腦模板提供較好的對位正規化空間。

我們的研究中，建立一個標準的建構腦模板流程，並針對特定族群所建立的客製化腦模板，提供一個更佳的對位空間。

誌謝

首要感謝陳永昇老師這兩年來的指導，研究所的兩年中，從老師的專業領域學習如何做好研究，老師常常告訴我們一些學習態度，也很關心學生平時的生活狀況並且時常鼓勵我們，此外也要感謝陳麗芬老師，在每次的討論中給我許多的建議，提供不同的研究思考或做法增加我研究的廣度，讓我的研究更加順利，在兩位老師的指導下，兩年的研究生活只能說我真的太幸運了。

另外要感謝這兩年曾經一起學習、玩樂和鼓勵的朋友們，無論是實驗室的學長姐、學弟妹、小助理們，亦或是實驗室外的同學和朋友，讓我的研究生活更充實有趣。最重要的當然還有一起同甘共苦的夥伴們，這兩年一起吃喝玩樂，熬夜努力，彼此打氣，謝謝大家帶給我兩年滿滿的回憶。

Construction of Customized Brain Template from Magnetic Resonance Images

A thesis presented

by

Kuo-Wei Lee

to

Institute of Computer Science and Engineering

College of Computer Science

in partial fulfillment of the requirements

for the degree of

Master

in the subject of

Computer Science

National Chiao Tung University

Hsinchu, Taiwan

2011

Construction of Customized Brain Template from Magnetic Resonance Images

Abstract

The magnetic resonance imaging (MRI) of brain images has been widely used to reveal the structure of human brain. A template space or template image provided a standard space to analyse brain structure or compare the differences among subject groups. However, large spatial transformation due to improper template space may lead to large artifact of brain structures in the warped brain image. Therefore, how to construct an unbiased brain template suitable for specific studies is essential to structural brain analysis.

The main purpose of this study aims at the development of a standard procedure for constructing MRI customized brain template. At first, we applied image analysis to all subject images to segment T1 image into different brain tissues. Secondly, we selected a reference image as the initial template space and applied an iterative registration procedure, including affine and non-rigid transformation, to gradually refined the template space and obtained a representative image. Then we spatially normalized all subject images to this representative image and averaged the warped images to obtain brain template.

This study constructed brain templates in Taiwan from 216 normal subject images (BTT216), including brain-only, whole-brain, grey matter, white matter, and cerebrospinal fluid templates. In addition, we constructed the template images for study-specific subject images, such as gender templates and different age-group templates. The evaluation method showed higher image correlation of warped images in BTT216 template rather than ICBM152 template. The average magnitude of deformation field was also shown in lower variation between BTT216 and subject images. The results of correlation shown in high similarity between study-specific template image and warped subject images which is normalized into the study-specific template space.

The customized brain template provides a better common space for brain structure analysis. The proposed method could be used as a standard procedure for brain template construction.

Contents

List of Figures

List of Tables

Chapter 1

Introduction

1.1 Background

1.1.1 Magnetic resonance imaging (MRI)

Magnetic resonance imaging (MRI) is a medical imaging technique, which is used in visualizing of the inside structure of organisms without physically intrusion. A magnetic resonance imaging instrument uses powerful magnets to polarize and excite hydrogen nuclei in water molecules in human tissue, producing a detectable signal which is spatially encoded resulting in images of the body. MRI provides high contrast between the different soft tissues of the body and commonly be used for studying the structure of human brain.

1.1.2 Brain Template

The structure of human brain is naturally different for each individual subjects. Different gender had been verified with variation in brain structure [16] [9]. Study of Good, Catriona D. et al. also showed the effectiveness of handedness [9]. The inter-ethnic difference of brain structure is confirmed by the study of Zilles et al. [23]. Besides, different nurture factors could also affect the individual structural variability, such as the effect with human growing [3]. The brain volume is growing from youth to young adult and the volume will start shrinking. Damage and disease may affect the brain structure,too [2].

The difference of MRI scanning environment could also obtained different images from different setting parameters of scanning machines. The MRI images could be in different dimensions or voxel size. In other words, the MRI images locate in different stereotaxic coordinate system with inconsistent orientation. Even we obtain the subject images form the same scanning machine with consistent setting parameters, the testing subjects may have a little movement in scanning process. This reason could also visualize the image in different orientation.

In order to the structure differences between each individual subjects from MRI, a standard stereotaxic coordinate system of human brain structural space should be provided. Re-

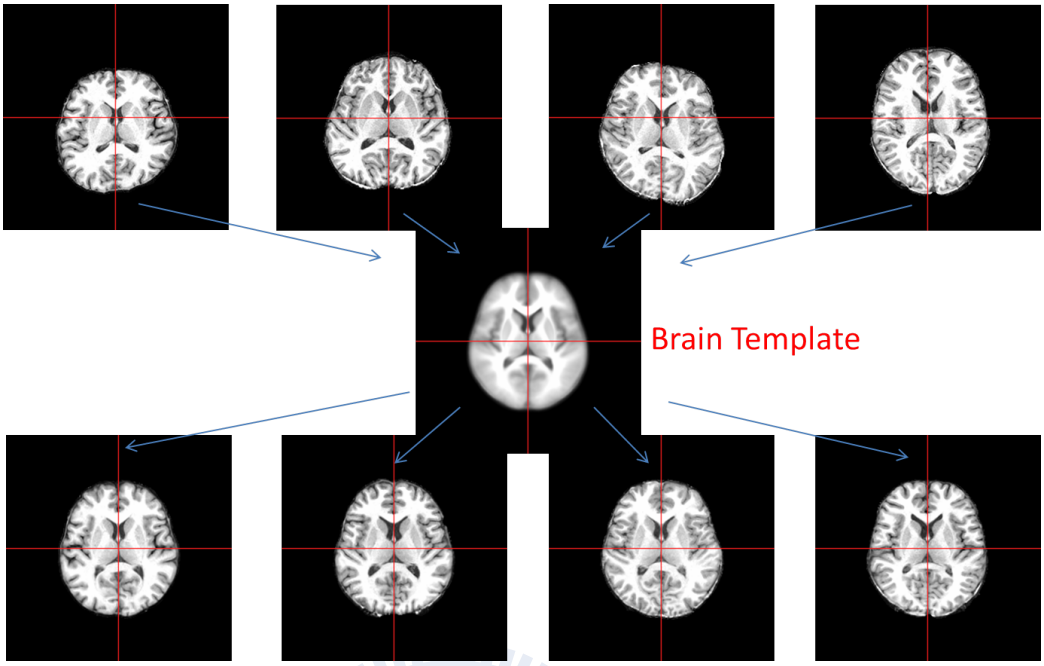

Figure 1.1: **Usage of template image.** To compare the different MRI images from scanning machine, template image provides a common space of structural coordinate system.

searchers could normalize each individual subject image to this template space as shown in Fig, 1.1 for further analysis or comparison. Due to the subjects may obtain from inconsistent sources or scan by different MRI machine environment and the brain structure of each subject may be affected by different nature or nurture factors. Each individual subject image from subject group should aligns to the same template space which is well-represented for that subject group. A proper represented template space could reduce the distortion from the registration procedure. Large distortion may increase the possibility of registration inaccuracy and bias the analysis result. Most researches apply the subject group images into the well-known template space, such as MNI305 and ICBM152. But these well-known template was constructed from the western subject images. We have already known that different ethnicity with significant difference of brain structure [23]. Constructing a reliable template space or template image have became an issue to study.

1.2 Related Work

Talairach atlas

In 1988, Talairach atlas was manually labeled of brain structure based on a 60-year-old French female [19]. This stereotaxic coordinate system manual is based on two landmarks, the anterior commissure (AC) and posterior commissure (PC). AC point is set as the orientation of the coordinate system. AC-PC line lie on the mid-saggital plane and also a straight line in horizontal direction. Fig 1.2 shows four slices of verticofrontal sections in Talairach atlas. As mapping to Talairach atlas, researchers also label AC and PC point on the subject image to do the initial alignment with rotation and translation.

Talairach atlas provides the structure coordinate system with relative location of brain structure in early year, but it also with some errors as template space. First, the atlas is biased to an individual elder woman. The image registration may contain large distortion for the variation from different structure of brain. Secondly, the registration to the Talairach atlas apply with manual landmark mapping which may contains the artificial error. On the other hand, the Talairach atlas assumes that the brain structure is symmetric, which seems to be irrational with the understanding of brain structure now.

MNI305

In 1992, Montreal Neurological Institute (MNI) created an average of 305 subject images mapping to the Talairach atlas called MNI305 [7] [15]. Fig. 1.3(a) displays the template image. This template created based on the coordinate system of Talairach atlas. The construction procedure consisted of two stages. At first, 241 brain images were registered to Talairach coordinates and averaged to become the first-pass image. The registration was achieved by aligning several manually-specified landmarks of 241 brain images together by 9-parameter linear transformation. In the second stage, 305 normal MRI scans were linear normalized to the first-pass image using automatic fitting strategy to reduce the artificial error.

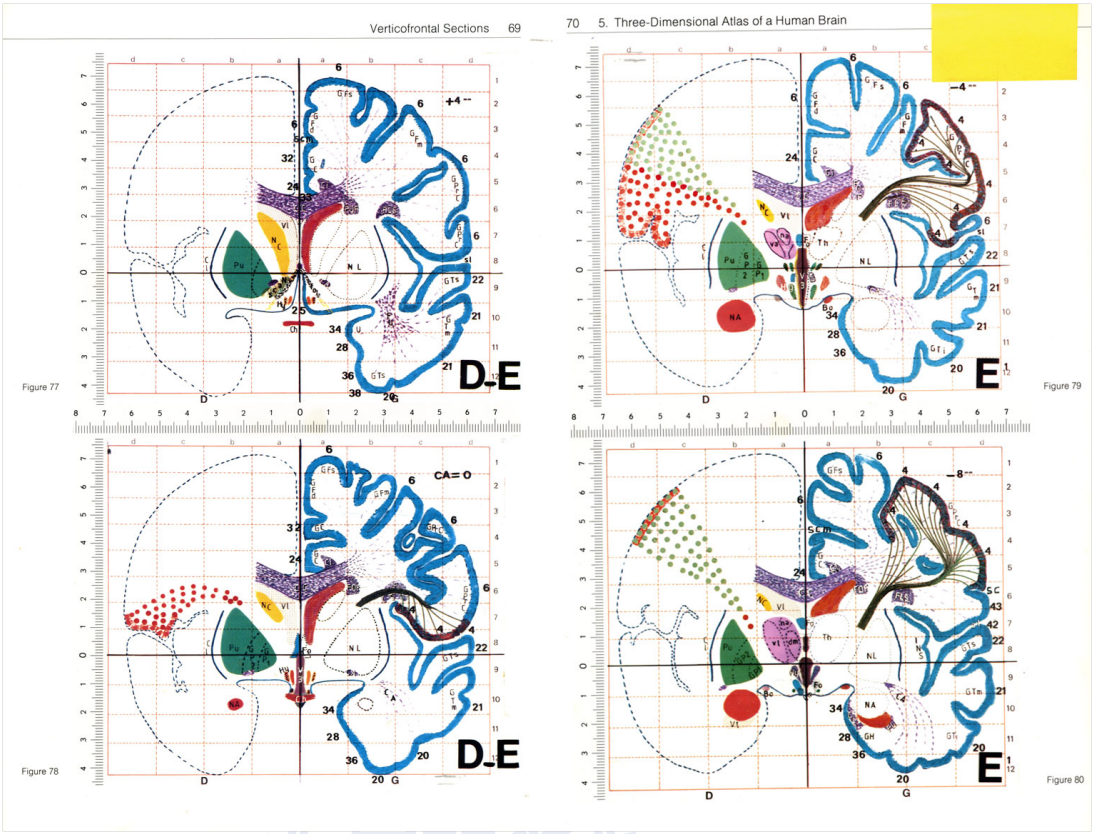

Figure 1.2: **Talairach atlas.** Talairach atlas of the human brain was introduced in 1988 by Talairach and Tournoux. They defined a standard coordinate system based on dissection of an 60-year-old French female's brain. This figure shows four slices of verticofrontal sections in Talairach atlas.
(Graphic source : http://homepages.nyu.edu/∼ef725/amygdala.html)

MNI305 template is obvious in low contrast from Fig. 1.3(a). The local structure could not been verified clearly (from Fig. 1.3(a)). It may attribute to the contrast of subject images or the registration technique did not provide high accuracy.

Colin27

To reduce the blurred condition of local structure from MNI305, a model was constructed by an individual subject - Colin Holmes, who had scanned 27 times within 3 months in 1998 [10]. The average image of these 27 images which normalized to MNI305

template shown in Fig. 1.3(b). Even Colin27 provided in high quality of template image, the template image is biased to this individual source object structure.

ICBM152 and ICBM452

In 1993, ICBM (International Consortium for Brain Mapping) was formed with four research sites: University of California, Los Angeles (UCLA), Montreal Neurologic Institute (MNI), University of Texas at San Antonio (UTSA), and the Institute of Medicine, Juelich/Heinrich Heine University - Germany. This ICBM projects is committed to develop a probabilistic reference system for the human brain. In 2001, The ICBM is template is wildly accepted as a standard template image which was constructed with 152 T1 normal subject images in higher contrast [14]. Each individual subject image was linearly registered to the MNI305 template and the average template image is constructed and shown in Fig. 1.3(c). The advantage of this template model is that it exhibits better contrast than MNI305 and also do not bias to any specific individual subjects. Followed by the improvement of techniques in MRI scanning and registration methods, ICBM still working on creating brain template. The registration method with non-linear technique has started to apply since 2002 and the building procedure has included six iteration times of registration which is show in Fig. 1.3(d) called ICBM152.

The ICBM template provides high resolution T1 images from age 19 to 90 in half males and females with high accuracy registration and still working on template construction. ICBM452 had published and constructed by 452 subjects. Even though, the template was constructed based on western human brain. As Zilles et al. had proved the inter-ethnic difference [23], we should not apply ICBM template as our common space of brain mapping and eliminate the possible of large distortion in image registration.

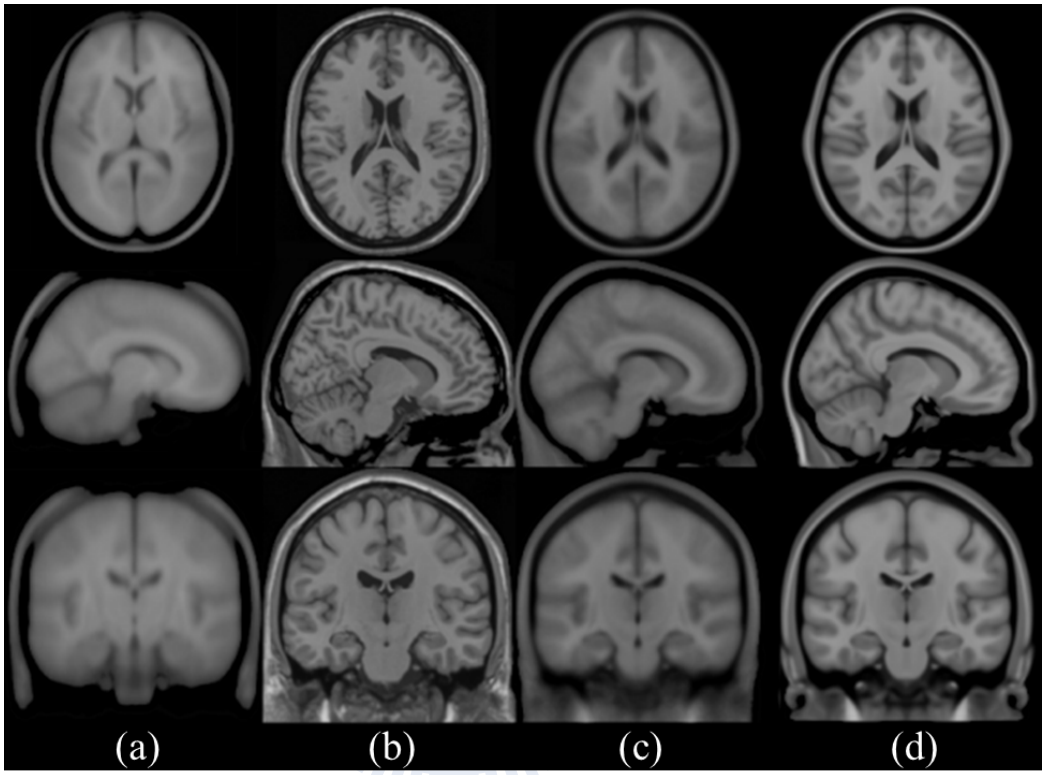

Figure 1.3: **Related well-know template.** (a) **MNI305** : Constructed by Montreal Neurological Institute (MNI) by averaged 305 normal subjects images mapping to Talairach atlas. (b) **Colin27** : Individual subject scanned 27 times within 3 months and averaged these 27 images which had normalized into MNI305. (c) **Affine ICBM152** : An averaged image with 152 higher contrast of subject images which were linearly registered to MNI305 by entirely automatic technique. (d) **ICBM152** : Improvement of Affine ICBM152 with nonlinear registration.
(Graphic source : http://www.bic.mni.mcgill.ca/)

Chinese Brain Template

In 2007, the group of National Taiwan University (NTU) constructed a Chinese brain template using their developed software by 10 subject images [21]. This study also verify the difference between the western brain template and Chinese brain template. Fig. 1.4 shows their template image. As the number of subject images was not large enough, the template image is obvious blurry. In 2008, the group of National Chiao Tung University (NCTU) constructed the averaged brain template in 191 normal subject images [6]. The construction procedure selected a representative image from the subject group as initial reference template image and used affine and non-rigid registration between reference image and the whole subject images to refine the template image. The results is shown in Fig. 1.4.

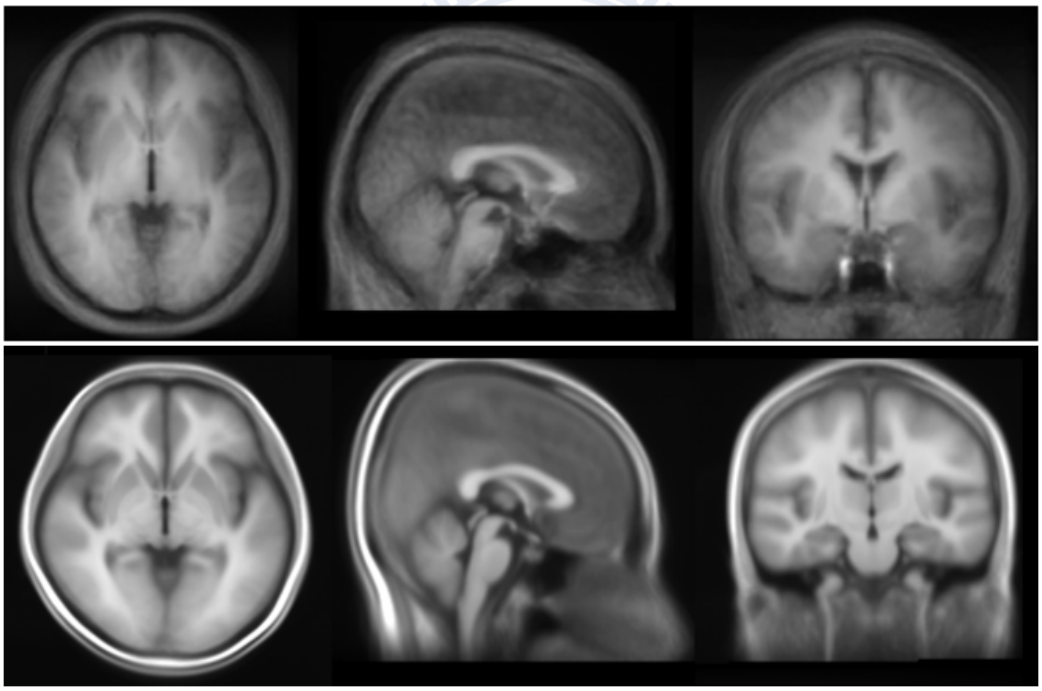

Figure 1.4: **Chinese brain template.** The upper figure shows the template constructed by NTU in 2007. The lower figure shows thetemplate constructed by NCTU in 2008.
(Graphic source : Upper : Wu, E. L et al. 2007. Lower : Chang, Y. Y et al. 2008)

1.3 Thesis Scope

This study aims to construct a standard procedure of creating customized brain template based on the subject images. Most construction procedure refer to the well-known template as initial template space, such as ICBM template [12] [8]. As the well-known template was constructed based on different ethnicity, the template constructed by Taiwanese subject images should be convinced for our study group. We select the initial reference image from our subject images which has the smallest variation to other subject images. Our construction procedure use iterative refinement to obtain the final representative image as our template space. In order to the bias from initial reference image, we acquired the brain template image by averaged all subject images mapping to the template space.

The construction procedure could be applied to construct the brain-only, whole-brain, grey matter, white matter and cerebrospinal fluid template image. Each template image applied the procedure of tissue segmentation at first and constructed on the same template space with the same deformation.

After constructed the procedure, we could implement the template on study-specific subject group, such as different genders or ages to construct male/female template image or template in different groups of age.

1.4 Thesis Organization

In the following chapters, we will present our construction procedure, experimental results, discussion and conclusion. In Chapter 2, we will describe our method of template construction and the evaluation method of our constructed template compared with different templates in Chapter 3. In Chapter 4, we will show the constructed template images and other experimental results. Then we will have a discussion about the experimental results in Chapter 5. Finally, in Chapter 6, we will make the conclusions.

Chapter 2

Proposed Methods of Brain Template Construction

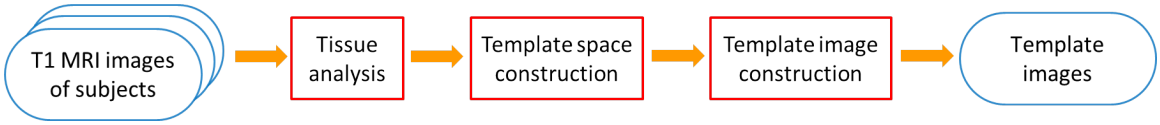

Figure 2.1: **Overview of template construction procedure.** The figure shows the brief flow chart of template construction.

2.1 Introduction

Our research seeks to provide a standard procedure of constructing MRI brain template image based on any study specific subject image groups. The researchers could construct the brain template depend on their demands of study. The procedure of construction does not rely on any well-known brain template to reduce the bias and differences between subject group and the reference template which constructed from different subjects. Our procedure includes three major procedures:

1. Tissue segmentation
2. Template space construction
3. Template image construction

Figure 2.1 shows the overview of our construction procedure.

At first, we obtain the raw data images with whole-brain from MRI scanning machine. To make sure the construction procedure have the best accuracy, all raw data in the subject group apply tissue segmentation. The procedures of tissue segmentation contain brain extraction to obtain the brain-only image which improves the accuracy of brain image registration; correction of intensity inhomogeneity solves the problem of non-uniform intensity in the same brain tissue to acquire the images with better quality; brain-tissue segmentation separates the brain volume into grey matter, white matter and cerebrospinal fluid.

Second, we apply the images acquired from the procedure of tissue segmentation to construct the template space and the construction procedure is based on the brain-only im-

ages. In the procedure of template space construction, we select an initial reference image as the initial template space. To refine this template space, we register all subject images to the template space and obtain an averaged transformation from these image registrations. The template space could be updated from an initial reference image into a representative image by applying the average transformation. The concept of refined the representative image could be performed in iterative registration. Iterative registration contain iterative affine registration and iterative non-rigid registration. Iterative affine registration refines the initial reference image with global shape of image and obtains an affine representative image. Iterative non-rigid registration refined the affine representative image with local structure alignment. The final representative image through the refinement of iterative affine registration and iterative non-rigid registration is our constructive template space. As we have the average transformation for each iteration time of registration based on brain-only images, the brain tissue and whole-brain images could also apply the same transformation and refinement to obtain the representative images of whole-brain and brain tissue.

Finally, the initial reference image iterative updates into a representative image which stands for the template space of the subject group images in brain-only and the procedure also obtain the template spaces of whole-brain and brain tissue. We register all subject images of different brain tissue into each template space and average the warped images. The averaged of warped images from subject images, which register to each template space are the template images. These template images could be used for structural analysis of human brain.

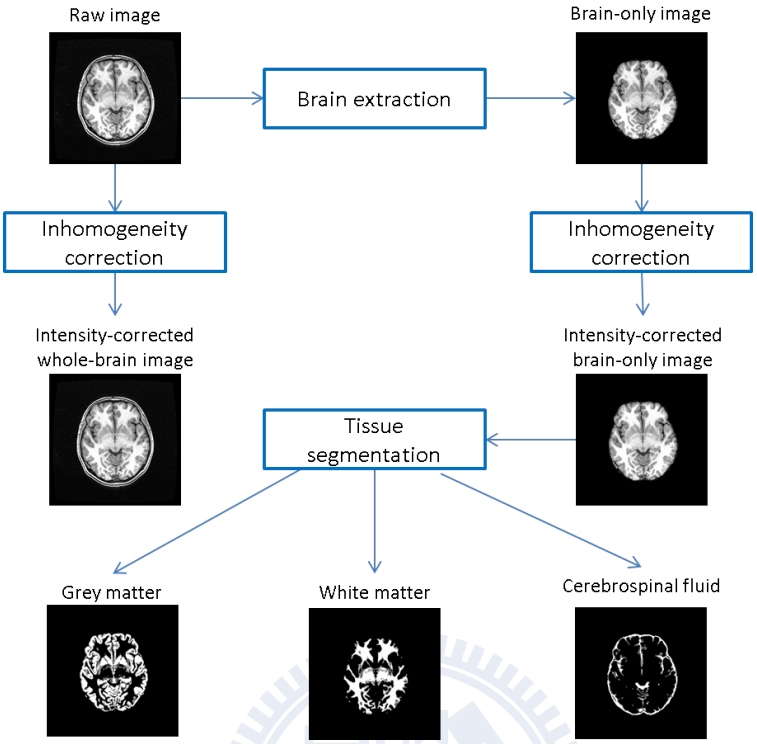

Figure 2.2: **Procedures of tissue segmentation.** The figure shows the flow chart of tissue segmentation. **Brain extraction**: Extracting the brain-only tissue improves the accuracy of brain image registration. **Inhomogeneity correction**: Non-uniform intensity correction is performed to acquire images with better qualities and contrast.**Tissue segmentation**: Separating the brain volume into three different tissues.

2.2 Tissue Segmentation

As MRI brain images obtained from the MRI scanning machine, there are some automatic procedures for tissue segmentation to help for the construction of template. Fig. 2.2 shows the flow chart with following procedures:

1. Brain extraction
2. Inhomogeneity Correction
3. Tissue segmentation

2.2.1 Brain Extraction

The raw MRI brain images provide the whole head information including brain skull, brain-tissue and other non-brain tissue. The brain skull and non-brain tissue may have the similar intensity level compared with brain-only image. To improve the accuracy of MRI brain image registration, the brain-only images support better image intensity information than whole-brain images [20]. In the procedure of template construction, we using the brain-only images to create the template space and template image. Before the construction procedure, each subject image apply brain extraction as the first step of tissue segmentation. Our research obtain the brain-only area using mri-watershed tool [17] acquired from FreeSufer which provided automated brain reconstruction tool from MRI by Athinoula A. Martinos Center for Biomedical Imaging. Both brain-only template image and whole-brain template image could be constructed form our template construction procedure.

2.2.2 Inhomogeneity Correction

MRI technique visualizes the image of brain structure by the different magnetic field gradients cause from the different atom of brain structure. The raw MRI image shows that the same brain tissue may visualize in different intensity, because same tissue of brain may not receive the same MR signal frequency practically. The reason is usually attributed to poor radio frequency (RF) coil uniformity and gradient-driven eddy currents [18]. Therefore, it will cause MRI image having intensity inhomogeneity in the same brain tissue area.

Due to intensity inhomogeneity, this study uses the technique of Non-parametric Non-uniform intensity Normalization (N3) [18] provided by Dr. A. C. Evans at the Montreal Neurological Institute to correct the problem. N3 optimizes the intensity field based on the distribution iteratively. The intensity correction applies in both brain-only and whole-brain images as shown in Fig. 2.3. Intensity correction could also improve the performance of image registration and brain tissue segmentation that both techniques base on the image intensity information.

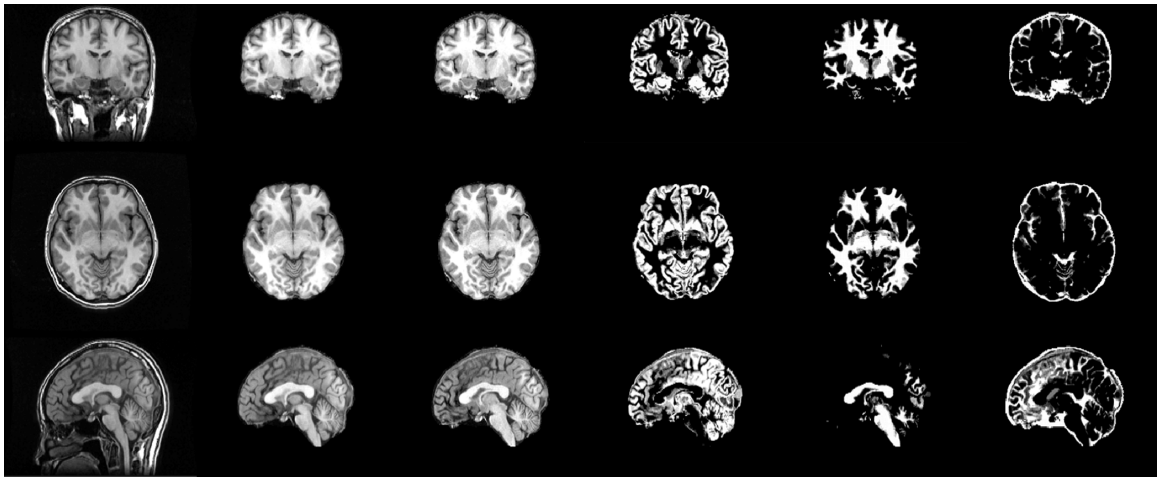

Figure 2.3: **Effect of the procedure of tissue segmentation.** This figure shows the effect from different tissue segmentation procedures in three different views of MRI brain image. From top to bottom are coronal view, horizontal view and sagittal view. From left to right are images of raw image; image with brain extraction; intensity correction after brain extraction; brain tissue of GM; brain tissue of WM; brain tissue of CSF. The brain tissue extracted from the brain-only image followed with correction of intensity inhomogeneity.

2.2.3 Brain Tissue Segmentation

Brain tissues general include grey matter (GM), white matter (WM) and cerebrospinal fluid (CSF). Different brain tissues contain distinct meanings in medical research. Therefore, grey matter, white matter and cerebrospinal fluid template image could also be constructed for specific research. The extraction tool or algorithm separate brain tissue into three parts based on image intensity. Therefore, the extraction step follows the correction result of intensity by N3 from the brain-only image. This study use the tool - FAST [22] (FMRIB's Automated Segmentation Tool) version 4.1 developed by University of Oxford Centre for Functional MRI of the Brain (FMRIB) to obtain the brain tissue.

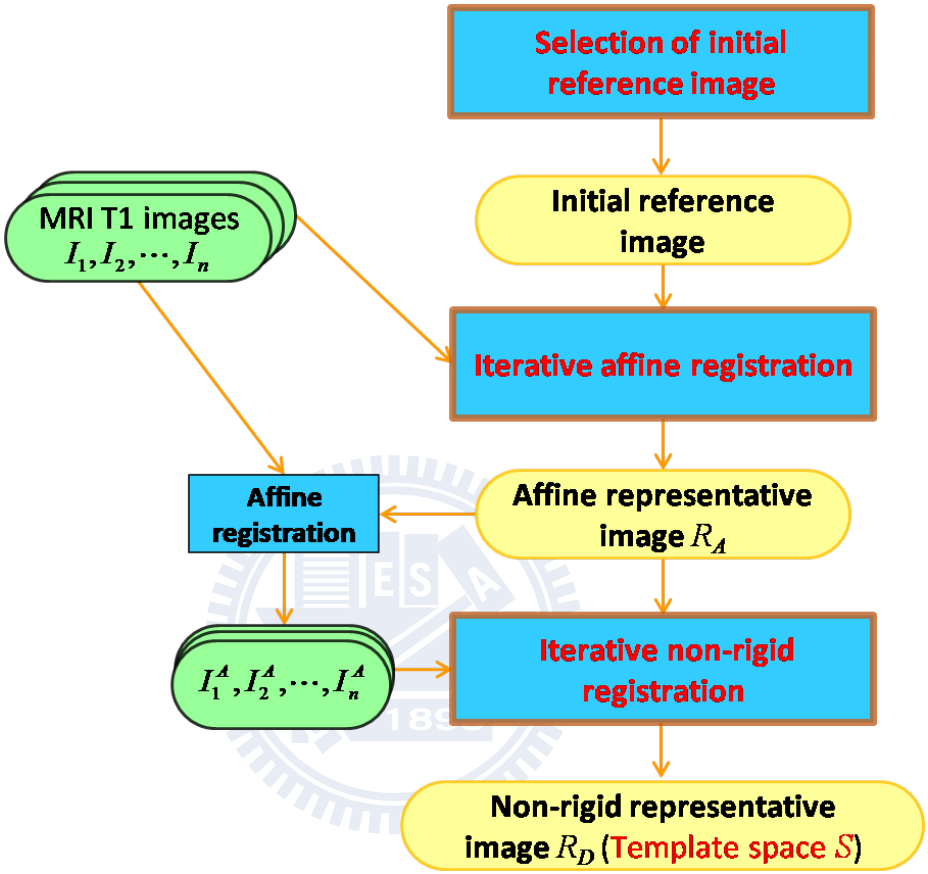

Figure 2.4: **Brief flow chart of brain template space constriction.** This flow chart shows the brief procedure of brain template space construction. The procedure with three major parts: **Selection of initial reference image**: Find a subject image from subject group which has the minimum variation to other subjects as initial reference image. **Iterative affine registration**: Use affine registration to refine the global shape of representative image of template space. **Iterative non-rigid registration**: Use non-rigid registration updating the representative image following the iterative affine procedure and refining the brain tissue structure.

2.3 Template Space Construction

In this study, we use MRI T1 brain-only images as input, because brain-only images provide better contrast of image registration than whole-brain image. All input images had been preprocessed by the steps described in the previous section of Chapter 2.2. The raw data image will do brain extraction at first, then solve the intensity inhomogeneity by N3 tool. Fig. 2.4 shows the brief procedure of creating customized template. The input subject group could be any customized subjects depending on specific study. An initial reference image will be selected from the subject group as a representative image of this group. Although the template will bias to the chosen one, iterative registration to construct the template should reduce the influence of the initial reference image. The construction procedure will create a representative image which represents for all the subjects from the subjects group. This representative image could also be seen as a template space. Any analysis or comparison could be implemented by normalize the subjects to this standard template space.

2.3.1 Initial Reference Image

The initial reference image is set as an initial template space for image registration. Most construction procedure choosed the well-known template such as ICBM152 as the initial reference [12]. Nevertheless, most well-known template was constructed from the Caucasians. The brain structure between different ethnicity was verified with inconsistency [23]. Choosing a representative image selected from the subject images as initial reference is also another choice [8]. The selection strategy in our study depend on the customized template which we want to construct.

As constructed the whole-subject template image, we choose an initial representative image from the subject images which has the lowest variance described below. The selection should reduce the bias rather than random selection from the subject images. To find this initial reference image R_0, we use pair-wise non-rigid registration to calculate the

variance of the magnitude of deformation field $D_{i,j}$ from source image i to target image j. Non-rigid registration aligns the local structure of brain image. More description of non-rigid registration will describe in Chapter 2.3.3. The following equation 2.1 shows the criterion of image selection:

$$R_0 = \arg\min_i \{var(\|D_{i,j}(x)\|) \mid \forall j \neq i,\ x \in \text{brain coordinate}\}. \tag{2.1}$$

Because the pair-wise non-rigid registration is very time consuming (for 216 subject images, the pair-wise registration cost about two months), we used the same initial representative image as in Chang [6] which was selected from 191 of the 216 subjects in our study according to the above-mentioned selection criterion.

When we construct the study-specific template, the whole-subject template image would is used as the initial representative image. The whole-group template not only can save the time of pair-wise image registration to find the image with the smallest variation but also can serve as a good initial template image to construct different study-specific templates. The comparison of study-specific templates should be more reasonable in this way.

2.3.2 Representative Image

This study aims to construct a customized template space and template image based on any demanding subject group which the researchers want to analyse. As we select an initial reference image being initial template space, the template construction procedure will refine the reference image into a representative image which is also the template space for the subject group. The representative image provides the template space information. After we construct the represented image (template space), all subject image could register to the template space and create the average template image. We use the brain-only image as our representative image rather than whole-brain image due to the similarity of intensity from the brain tissue and brain skull. Because brain registration is based on the intensity of brain image, the brain-only image provide higher registration accuracy. Even only the brain-only image will be considered as the target to be refined, other brain image obtained

from the preprocessing steps could also apply the same refined transformation and construct the template. The result types of representative image will include brain-only, whole-brain, grey matter, white matter and cerebrospinal fluid images.

2.3.3 Image Registration

The image registration based on the transformation of each voxel from source image to target image. The registration process includes two major parts: global affine normalization T_A and non-rigid transformation T_N. Affine registration do the global shape alignment. Non-rigid registration do the alignment of local structure of brain. The effect of different registration methods shows in Fig. 2.5. For each grid point p in source image and correspond location q in target image, the following equation present the transformed relation:

$$q = T_A(p) + T_N(T_A(p)) \tag{2.2}$$

Affine Registration

Affine normalization aligns the global shape from the source image to the target image with 12 transform parameters including translation (t_x,t_y,t_z), rotation (θ_x,θ_y,θ_z), scaling (s_x,s_y,s_z) and shearing (k_{xy},k_{xz},k_{yz}) for each contains in three directions. For Each grid point p of source image maps to the corresponding location q in target image, the transformation could use a transform matrix M to present the mapping relation. The relation is shown in equation 2.3 and the matrix M also shown below. In this study, University of Oxford's FMRIB Software Library (FSL) provided FMRIBs Linear Image Registration Tool (FLIRT) [11] which be used in the procedure for affine registration.

$$q = T_A(p) = Mp \tag{2.3}$$

and the transform affine transformation matrix M with a rotation matrix R_{xyz}:

$$M = \begin{bmatrix} 1 & \mathrm{k}_{xy} & \mathrm{k}_{xz} & 0 \\ 0 & 1 & \mathrm{k}_{yz} & 0 \\ 0 & 0 & 1 & 0 \\ 0 & 0 & 0 & 0 \end{bmatrix} \begin{bmatrix} \mathrm{s}_x & 0 & 0 & 0 \\ 0 & \mathrm{s}_y & 0 & 0 \\ 0 & 0 & \mathrm{s}_z & 0 \\ 0 & 0 & 0 & 1 \end{bmatrix} \begin{bmatrix} & & & 0 \\ & R_{xyz} & & 0 \\ & & & 0 \\ 0 & 0 & 0 & 1 \end{bmatrix} \begin{bmatrix} 1 & 0 & 0 & \mathrm{t}_x \\ 0 & 1 & 0 & \mathrm{t}_y \\ 0 & 0 & 1 & \mathrm{t}_z \\ 0 & 0 & 0 & 1 \end{bmatrix}$$

$$R_{xyz} = R(\theta_x)R(\theta_y)R(\theta_z)$$

Non-rigid Registration

Non-rigid registration mainly solves the problem of inter-brain tissue misalignment after we align the global shape of image from affine normalization. The spatial mapping used in our study is based on a set of Wendlands radial basis functions (RBFs) with different levels of support extents [13]. RBFs model the deformation field D of the brain image from source image to target image. The following equation 2.4 shows the relation of mapping from source image to target image.

$$q = T_N(T_A(p)) = p + D(p) \tag{2.4}$$

In the evaluation of image registration from a source image to a target image, each coordinate location in the deformation field represents the deformation vector with the magnitude and direction of deformation. By the average and variance of magnitude, we could observe the variation between source image and target image. We could also use the deformation field to evaluate the accuracy of image registration.

2.3.4 Iterative Registration

The initial selected reference image is seen as the first representative image for the subject group because it has the minimum variance with other subject images. Nevertheless, the template space will bias to this selected one if we construct the template at the selected

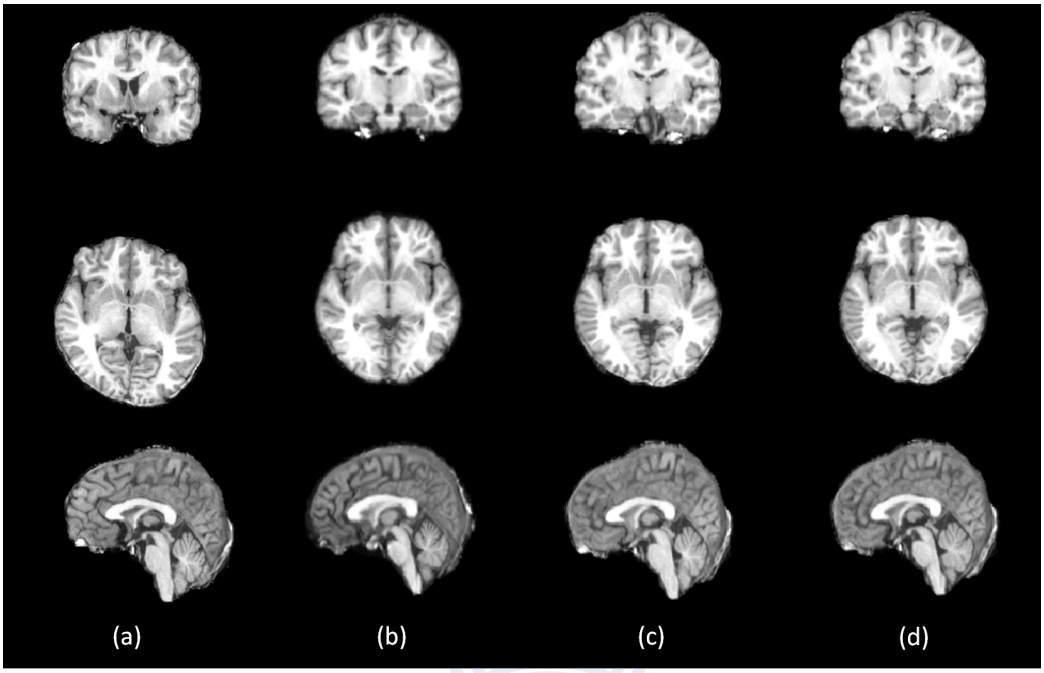

Figure 2.5: **Display of image registration with affine and non-rigid registration.** (a) Source image. (b) Target image. (c) Mapped from source image into target image by affine registration. (d) Apply non-rigid registration from (c) to (b). In other words, mapped source image into target image with affine registration and non-rigid registration.

space. The procedure of constructed template in iterative registration could refine the template space and reduce the influence of initial reference image. The constructed procedure is shown in Fig. 2.6 in iterative steps.

At first, initial reference image R^0 is selected from the subject group. Without using averaging subject group images as initial image, the individual MRI scan image provides better contrasting information and clearer brain anatomical local structures. This could make registration parameters and cost functions more precise and increase the accuracy of registration. Using automatic registration method, this reference image could optimize to become a representative image.

The creating procedure of registration divides into affine registration part and non-rigid registration part. In affine registration, all subject images will do translation and rotation to the initial template space at first because the subject may have a little movement when

they did MRI scanning. It should not be considered as the factor of inconsistent of brain structure. After the alignment with translation and rotation, the reference image maps to each subject images in affine registration with scaling and shearing, which solves the problem of global shape difference. The registration procedure in iteration i will obtain n subjects' transform matrices M_j^i where j from 1 to n which including the difference information between the reference image and each subject. As we want to optimize the reference image to be a well representative image of subject group, this purpose could implement by applying the average transform matrix $\overline{M}$ on the reference image to update the reference image R_A (Equation 2.5). The affine registration with scaling and shearing could do iteratively and the representative image will refine iteratively until steady. This concept could also be used in non-rigid registration for alignment of local structure. The updating representative image R_A from the iterative affine registration could be the initial as the non-rigid registration. The non-rigid registration deformation field, D_i handles the inter-brain alignment. The iterative non-rigid registration procedure is similar to affine registration as in equation 2.6. The representative image could be updated iteratively until in a steady state R_D. The final representative image R_D is also the final determinative templates space S.

$$R_A^{i+1} = \overline{M^{i+1}} \times R_A^i \qquad \text{for } \overline{M^i} = (\sum_{j=1}^{n} M_j^i)/n \tag{2.5}$$

$$R_D^{i+1} = \begin{cases} R_A + \overline{D^{i+1}}(R_A) & \text{if } i = 0 \\ R_D^i + \overline{D^{i+1}}(R_D^i) & \text{if } i > 0 \end{cases} \qquad \text{for } \overline{D^i} = (\sum_{j=1}^{n} D_j^i)/n \tag{2.6}$$

2.3.5 Stopping Criterion

For each iteration, the representative image R^{i-1} is refined to a new representative image R^i. The iteration of this representative will converge into a stable state. In general, iteration times should be stopped in finite iterations. As the average affine transformation matrix or average deformation field in a stable state, transformation for the image would be slight and small. In other words, the variance of the intensity of representative image

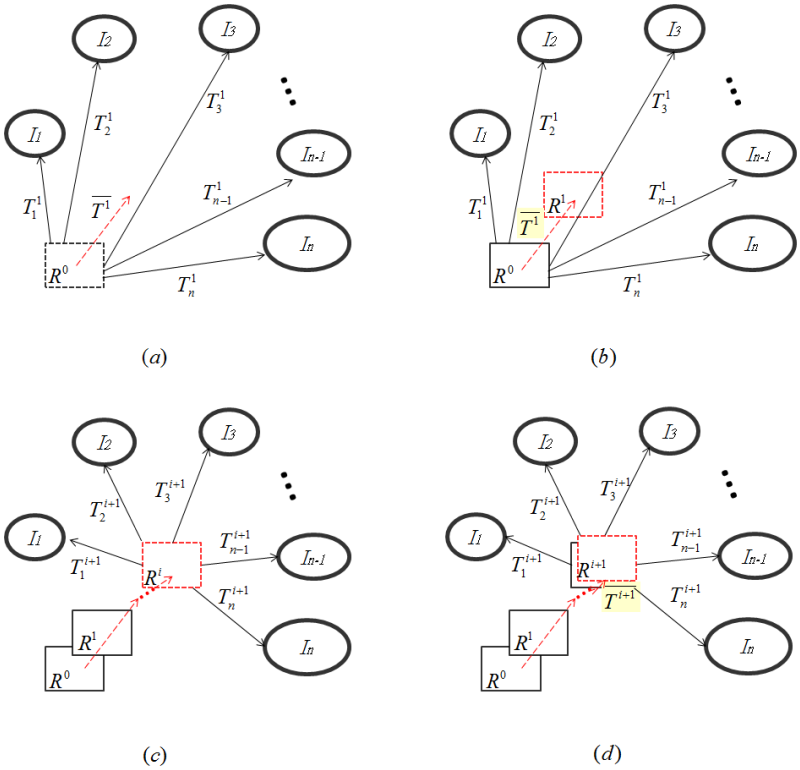

Figure 2.6: **Iterative refine representative image.** This flow chart shows updating procedure for represented image from (a) to (d). R : representative image; I : individual subject image; T : transformation of registration (As in affine registration, T should be a affine transformation matrix M. In non-rigid registration, T would be deformation field D); $\overline{T}$: average of transformation; i : iteration time; n : subject numbers.

should be stable. At first the average intensity difference ID per voxel would be computed and recorded shown in equation 2.7. Each value shows the extent of variation in iteration time of $i-1$ and i.Due to the registration will not steady, the image intensity still have a little different. We set the slope of average voxel intensity difference ID^i as the threshold for stopping iterative registration. Equation 2.8 shows the slope $IDP^{(i,i+1)}$ of difference between ID^i and ID^{i+1}

$$ID^i = (\sum_{j=1}^{k})|R_s^i(x_j, y_j, z_j) - R_s^{i-1}(x_j, y_j, z_j)|)/k \tag{2.7}$$

$$IDP^{(i,i+1)} = (ID^i - ID^{i+1})/ID^i \tag{2.8}$$

2.3.6 Image Interpolation

For image registration, the output will obtain an affine transformation matrix M in affine registration or a deformation field D in non-rigid registration. The transformation estimate the mapping from location of source image into the corresponding location in target image. The warped image will be created by the technique of image interpolation. In affine registration, we transform the source image into target image space by applying affine transformation matrix using FLIRT [11]. In non-rigid registration, the deformation filed is not a grid point to grid point mapping. In other words, each grid point of source image may not actually map to a grid point in the target image as in Fig. 2.7 of Step 1. We will use following method to do interpolation and create the warped image.

The interpolation steps are shown in Fig. 2.7. To construct the target image, the intensity information from source image is necessary. Due to the mapping relation from the deformation field, we obtain the intensity information from the grid point in source image and the mapping location in target image. Then we will have the information of the intensity in target image even non-uniform distribute in the target image coordinate. To obtain the value of each grid point in target image, the concept of our interpolation method is used intensity and distance value of nearest neighbors. How to find the nearest neighbors without searching for the whole-image becomes an issue.

At first, considering a grid point T in target image and find a close location S' deforms from a grid point S of source image. In source image, set the grid point S as center and find a cube contain enough grid point for interpolation. Collected these grid point into the set G as in Fig. 2.7 of Step 2. The size of the cube may be variant depends on the numbers of neighbors we needed. In this study, we use nearest eight neighbors for image interpolation. After found a set G of grid points from source image, G' record the coordinate location form the deformation field D in target image. From set G', select eight nearest neighbors and calculate the value of grid point T (Equation 2.12) using the inverse from distance as

weighted (Equation 2.11).

$$G = \{(x_j, y_j, z_j) \mid i = 1, ..., n\} \tag{2.9}$$

$$G' = \{D(x_j, y_j, z_j) \mid i = 1, ..., n\} \tag{2.10}$$

$$w(x_j, y_j, z_j) = 1/dist(D(x_j, y_j, z_j), T) \tag{2.11}$$

$$v(T) = \frac{1}{\sum_i w(x_i, y_i, z_i)} \sum_i w(x_i, y_i, z_i) \times v(x_i, y_i, z_i) \tag{2.12}$$

2.3.7 Image Outlier Removing

The construction procedure input all needed subject images to create the template space and template image. If one of the input image with great deform form representative image to this one, the result template may affect by this outlier especially when the subject numbers are not large enough. To ensure the template could not only represent the subject group but also be in a standard coordinate system, the procedure should add criteria to remove the outlier of subject image.

In this study, the outliers consider transformation effect from scaling and shearing in affine transform. Translation and rotation align two images to the same coordinate space. Deformation of non-rigid registration reduces the brain tissue structure difference. The last two effects are not stand as outlier generally. Both scaling and shearing include 3 directions: Scale with x-axis, y-axis and z-axis, shear parallel to the x-axis by variable of y and z and shear parallel to the y-axis by variable of z (Figure 2.8(a) from left to right).

There are total six variables considered as outlier factors. Each registration between subject and representative image will obtain those six variables. Compute average and standard deviation for six outlier factors in each iteration time of affine registration. If any factors of the six variables out of range: average five times standard deviation in second and third iteration time, the subject will set as outlier. If any factors out of range: average four times standard deviation in fourth and fifth iteration time, the subject will also set as outlier. Finally, the criteria will set outlier which variable of factor is out of range: average

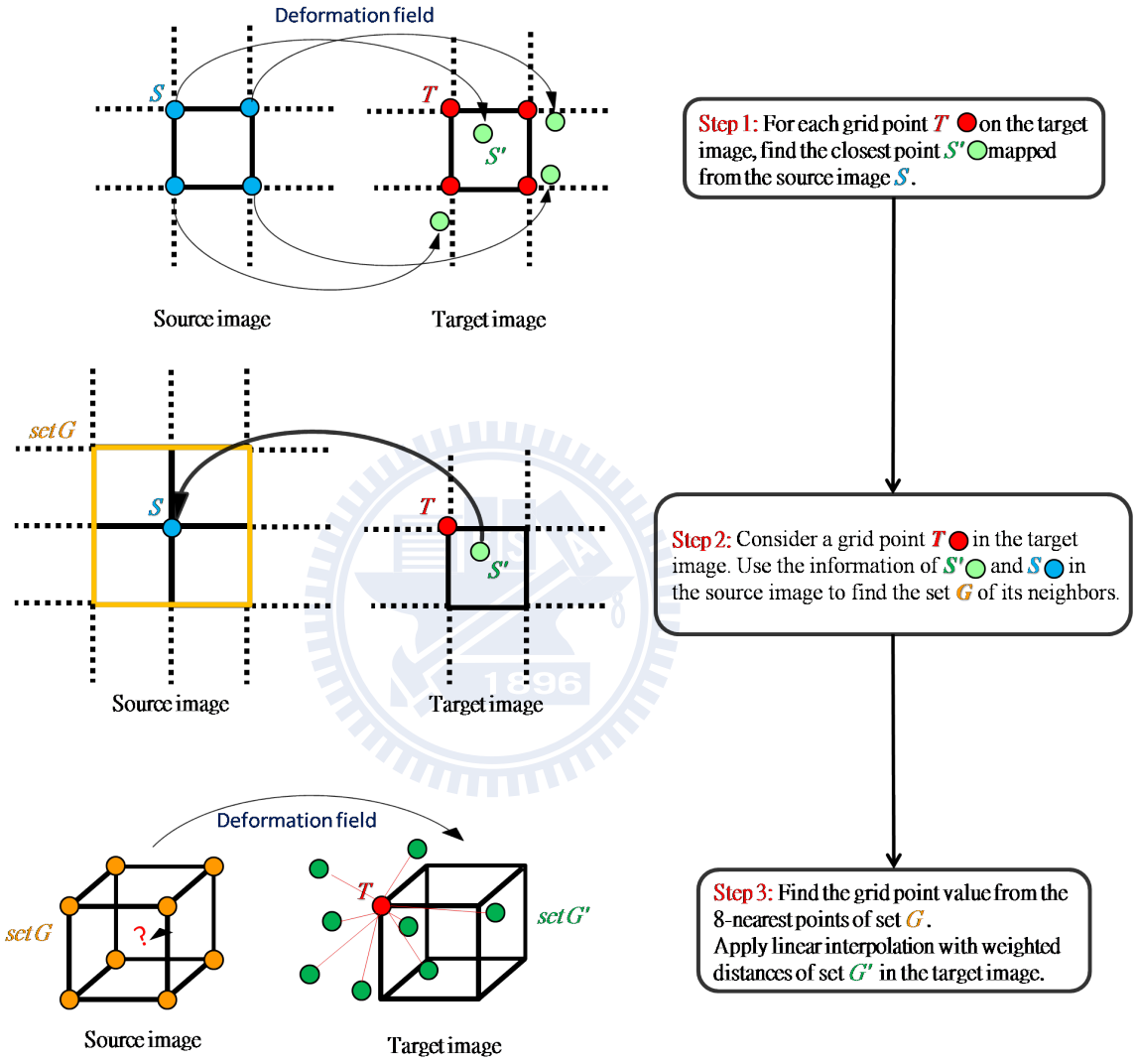

Figure 2.7: **Steps of image interpolation.**

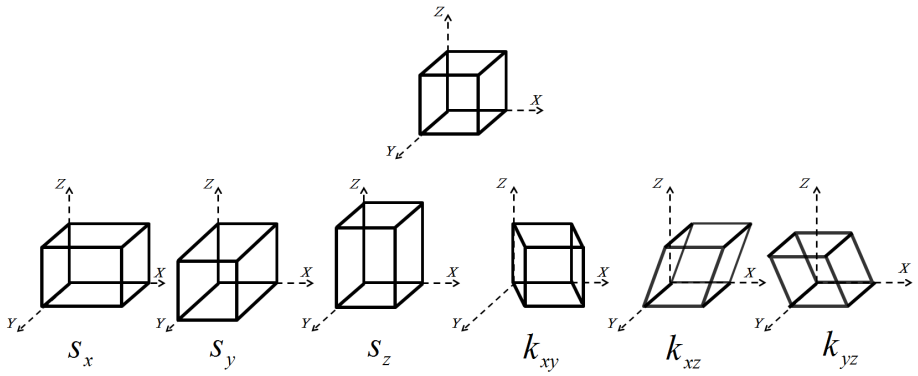

(a)

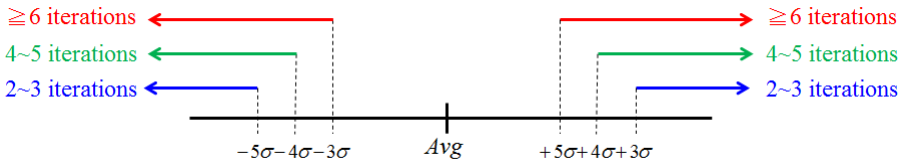

(b)

Figure 2.8: **The outlier factors and outlier criteria**: (a)**The outlier factors**:Here are the considering outlier factors(coefficients) from affine registration which include scale in x,y,z-direction (s_x,s_y,s_z) and shear parallel to the x-axis by variable of y and z (k_{xy},k_{xz}) and shear parallel to the y-axis by variable of z (k_{yz}) (from left to right). (b) **The outlier criteria**: The blue line shows the outlier range in 2_{nd} and 3_{rd} iteration time. The green line shows the outlier range in 4_{th} and 5_{th} iteration time. The blue line shows the outlier range after 6_{th} iteration time. The range is defined by the average value ($Avg.$) and standard deviation (σ) in each of outlier factors.

three times standard deviation above sixth iteration time. The range setting also shows in Fig. 2.8(b).

2.4 Template Image Construction

2.4.1 Customized Brain Template

The iterative registration refine the initial reference image into a representative image which represents the template space for subject group. The template space provides the

coordinate information of local brain structure. We could transform all the subject images into this template space and average all warped images. The averaged image could provides the coordinate information of local brain and also information of whole-brain structure from all subject images.

2.4.2 Whole-brain and Brain Tissue Template

The construction brain template procedure based on the brain-only images. Each iterative registration obtain the average affine transformation matrix or average deformation field. We could apply these transformation on the whole-brain, grey matter, white matter and cerebrospinal fluid to obtain the brain tissue template space and template image. The application of averaged transformation in i times of iteration shows in equation 2.13 and equation 2.14. Fig. 2.9 shows the procedure of constructing whole brain and brain tissue template.

$$R_A = \overline{M^{i+1}} \times \overline{M^i} \times \cdots \times \overline{M^1} \times R_A^0 \tag{2.13}$$

$$R_D = R_A + \overline{D^{i+1}}(\overline{D^i}(\cdots \overline{D^1}(R_A))) \tag{2.14}$$

2.5 Construction of Study-specific Template Image

In addition to the template constructed for whole subject images, we can also construct the templates based on study-specific images. In this study, we considered different genders and ages of subject images to create the male template, female template, and templates in six different age ranges.

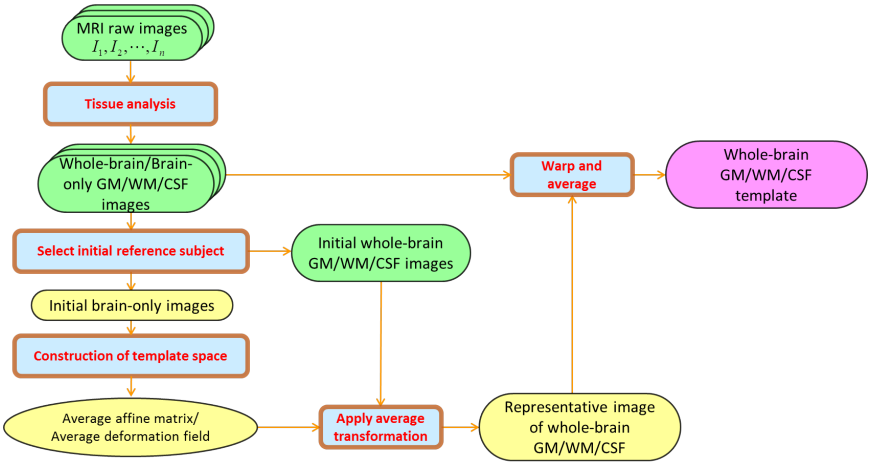

Figure 2.9: **Brief flow chart of brain-tissue template construction.** This flow chart shows the brief procedure of brain-tissue template construction. The procedure of original template construction obtain the average affine transformation matrix and average deformation field as the first column. The whole-brain and brain tissue image could apply the same transformation to obtain the template space. All subject specific images transform into the template space and get the averaged template image.

Gender templates

The construction of male/female template creates from the whole male/female subject images. The whole-subject template image is chosen as the initial reference template as the initial of the representative image. The construction procedure is the same as the construction of the whole-subject template image which iteratively updates the representative template image.

Age-group templates

The whole subject images were divided into six groups each with 10 years according to the ages of subjects. The ages in the youngest group range from 14 to 19, and those in the oldest group range from 60 to 69. Each specific age-group templates was created only from the subject images with the specific age range. For the construction procedure of each template, the whole-subject template image was used as the initial representative image.

2.6 Detailed Flowchart of Brain Template Construction

Fig. 2.10 shows the detailed flowchart of brain template construction. It mentions all the methods described in the previous of this chapter.

Figure 2.10: **Detailed Flowchart of Brain Template Construction.** This figure shows the whole procedure of template construction which combined with three major parts of procedure: data analysis, template space construction and template image construction and each with detailed flowchart.

Chapter 3

Evaluation of Brain Templates

3.1 Introduction

As the template space and template image are constructed, there are some evaluations for testing our constructed template is well-represented as the subject groups. The comparison is focus on the difference between the template image and the subject image warped into the template space. As the difference is lower or the warping magnitude is smaller, the template had better representativeness. The well-known template could also be a comparison to make sure our constructed customized template is better. The template evaluation could be based on the following two factors:

1. The intensity of brain image

2. Deformation field from non-rigid registration

3.2 Evaluation Using Image Intensity

Considering the image intensity value, if the brain template is well-represented for the whole subject group, the close voxel coordinate between each subject images which have mapping into template space should have similar intensity value. The whole subject group images transform into our creating template space to do the following evaluative methods. This study uses intensity standard deviation for each voxel in warping image and intensity correlation for each warping image to evaluate the performance of our template.

Intensity standard deviation

For measuring the variance between warped images and template image in each coordinates, we consider the intensity of the same voxel coordinate between all warped images which obtain from all subject images register to the template space. If the template image improves the accuracy of registration, the intensity value of different warped images in the

same voxel coordinate should be close. Equation 3.1 shows the computing formula.

$$SD(x) = \sqrt{\frac{1}{n}\sum_{j=1}^{n} I_j^S(x)^2 - (\frac{1}{n}\sum_{j=1}^{k} I_j^S(n))^2} \tag{3.1}$$

n is the subject number and $I_j^S(x)$ stands for the intensity of subject j in template space S at coordinate x.

Small standard deviation represent all image transform to this template space in closer divergence. Because this measure is focused on the variance of each voxel coordinate, the result could also show where the larger difference is in which brain tissue structure.

Image correlation

Another measuring method computed the correlation between subject images and template image. Correlation shows the similarity of two images and equation 3.2 shows the computing formula.

$$r_{AB} = \frac{\sum_{i=1}^{k}(A_i - \overline{A})(B_i - \overline{B})}{\sqrt{\sum_{i=1}^{k}(A_i - \overline{A})^2 \sum_{i=1}^{k}(B_i - \overline{B})^2}} \tag{3.2}$$

As A and B are two images, A_i (or B_i) stands for the intensity value of image A in coordinate i. k is the voxel number of image without background (image intensity equals zero). In this study, we perform the correlation value between the averaged template image and the warped image which transform from an individual subject image into template space. If the template image could provide better registration accuracy, all warped subject images will have high similarity with the template image.

Correlation value is located from zero to one. If the correlation closer to one, the similarity between this two images are higher. In other words, the template image is representative as the subject image.

3.3 Evaluation by Deformation Field from Non-rigid Registration

Study of the displacement information stored in the deformation field is also another evaluation method. The deformation field was obtained by non-rigid registration. The magnitude from the deformation field shows the divergence between the template and each individual subjects. As the aim purpose is constructed a well customized template, this template image should represent the subject group and provide a standard space for image registration. Smaller deformation field provide higher registration accuracy with smaller distortion in image registration [12]. We could compute the average deform magnitude of vector and the variance of this magnitude to observe the difference between subject image and template image.

Magnitude of Deformation Field

Non-rigid registration procedure will obtains 3-dimension deformation field in millimeters. Each coordinates' deform magnitude will perform in Euclidean distance.The average deform magnitude will consider each coordinates in whole image without the background (intensity value equals zero). The average deform magnitude AD is performed by following equation:

$$AD = \frac{1}{k}\sum_{i=1}^{k}\sqrt{(D_{x_i})^2 + (D_{y_i})^2 + (D_{z_i})^2} \tag{3.3}$$

D_{x_i}, D_{x_i}, and D_{x_i} represent the deform vector of coordinate i in direction x, y, and z. k present the considering voxel numbers. The average could be focused on a voxel coordinate or the whole image, so the number of k may be variant.

The average deform magnitude of whole image shows the difference between the template space and subject group. The average on each coordinates show the difference of register distance for local tissue structure. This display could also show the major part of brain tissue registration by non-rigid registration of brain.

Variance of Deformation Field

By observing the variance of non-rigid deformation field, we can know the anatomically regional variability of the difference between the template and individual brains. However, a good template should cause not only small distortion magnitude of deformation but also small distortion variance. When the variance of non-rigid deformation field is zero, this template is called unbiased to the individual brains. For calculating the variance, when we normalize subjects to the template, the deformation magnitude of each voxel is recorded. We calculate the variance of all magnitudes in the same voxel of all brain images. Finally, we obtain the topography of variance of non-rigid deformation field.

In addition, we use another evaluation method based on the deformation field acquired from image registration. We manually label six landmarks for each subject images. Table 3.1 shows these six landmarks and the labelled position. Fig. 3.1 shows the position of each landmarks in sagittal view. We could calculate the variance of the magnitude of deformation on the same landmark for all subject images when registered into different template images. Based on the variation of specific location of brain structure, the variance of the magnitude of deformation could verify whether the brain template is similar to the subject images or not.

Tissue Name	Labelled Position
Anterior commissure (AC)	Superior and posterior margin
Posterior commissure (PC)	Inferior margin
Genu (GU)	Inferior margin
Thalamus (TH)	Inferior margin
Splenium (SP)	Inferior margin
Cerebellar (CB)	Superior margin

Table 3.1: **The landmark labelled position.**

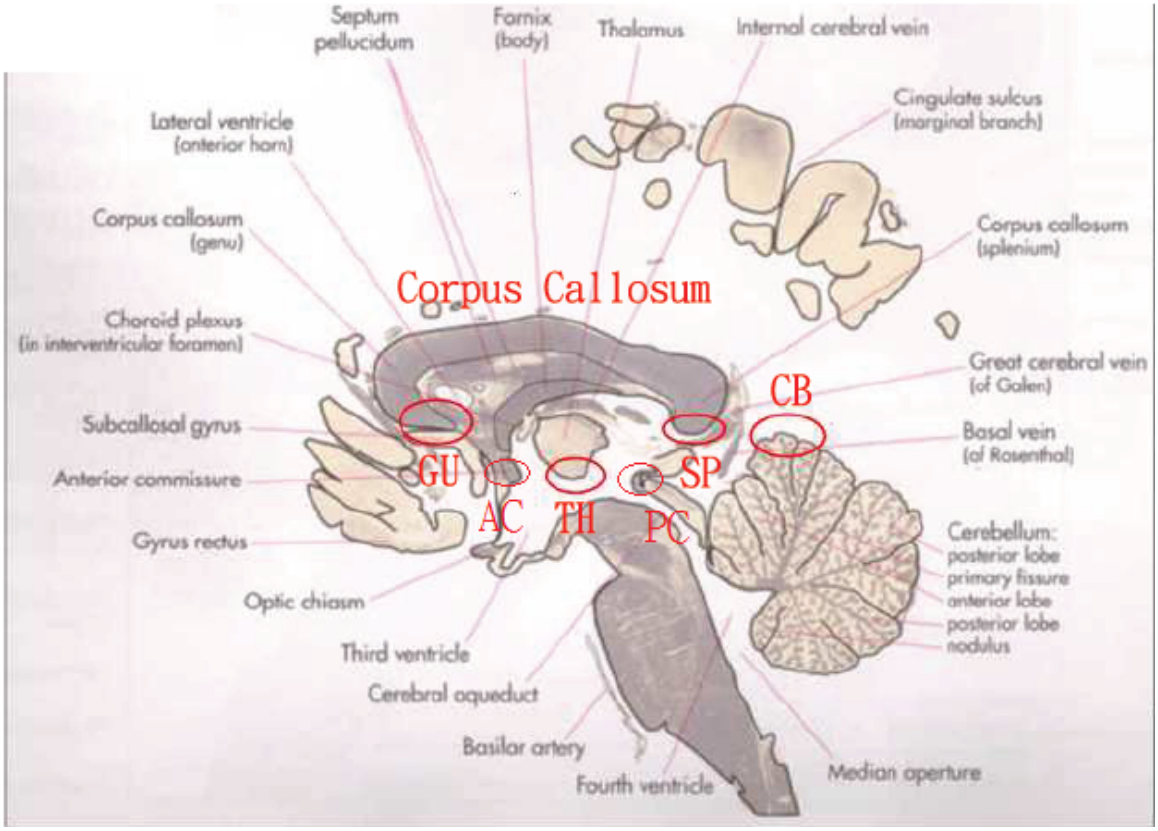

Figure 3.1: **Landmarks.** The figure shows six landmarks including anterior commissure (AC), posterior commissure (PC), Genu (GU), Thalamus (TH), Splenium (SP), and Cerebellar (CB).

Chapter 4

Experimental Results

4.1 Materials of MRI Brain Images

The MRI scans are obtained from Integrated Brain Research Unit (IBRU) of Taipei Veterans General Hospital. The MRI images were acquired on a 1.5 Tesla GE MR scanner, using 3D-FSPGR pulse sequence (TR = 8.67 ms, TE = 1.86 ms, TI = 400 ms, NEX = 1, flip angle = 15°, bandwidth = 15.63 kHz, matrix size = $256 \times 256 \times 124$, voxel size = $1.02 \times 1.02 \times 1.5$).The subject group includes 86 males and 130 females in total 216 normal subjects. Age range is from 4 to 69. Table 4.1 and 4.2 show the statistical data of database. In this research, we transform the raw data from the scanning machine into Analyze format and use T1 MRI brain image as our study image groups.

	Age Group						
	14-19	20-29	30-39	40-49	50-59	60-69	Total
Male	5	44	13	13	11	0	86
Female	14	35	31	20	26	4	130
Sum	19	79	44	33	37	4	216

Table 4.1: **Number of subjects from the database.**

	Age		
	Male	Female	Total subjects
Mean	32.4651	36.5000	34.8935
Std.	11.8716	13.086	12.743

Table 4.2: **Average and standard deviation of age from the database.**

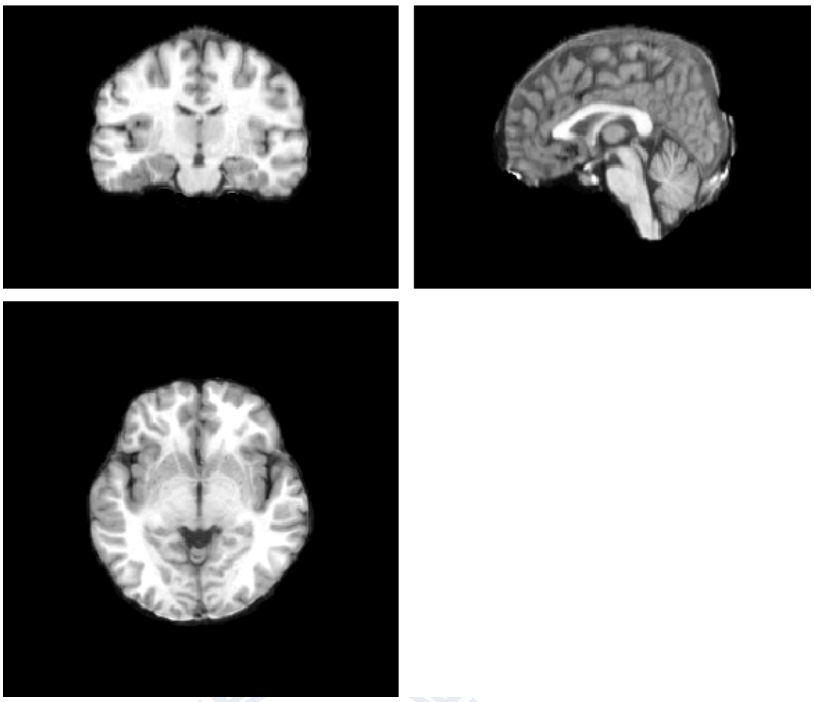

Figure 4.1: **Initial reference subject image.** In our template constructed procedure. This figure shows the selected female subject in 23 years old. The figure shows in coronal view (upper left), sagittal view (upper right), and horizontal view (lower left).

4.2 Construction of Brain Templates

4.2.1 Representative Brain Image (Template Space)

By the procedure of construction of customized template, we select a subject image which has the minimum average deformation field of magnitude to other subjects as the initial reference space. Fig. 4.1 shows the selected 23 yeas old female subject image in our procedure. In the iterative registration, we will obtain a representative image from iterative affine registration which represents the global shape aligned space for the input subject group and then a representative image combined with iterative non-rigid registration which stand for the template space of the input subject group. Non-rigid iteration deal with the problem of local brain tissue alignment. Fig. 4.2(a) shows the representative obtained from iterative affine registration and Fig. 4.2(b) with additional iterative non-rigid registration.

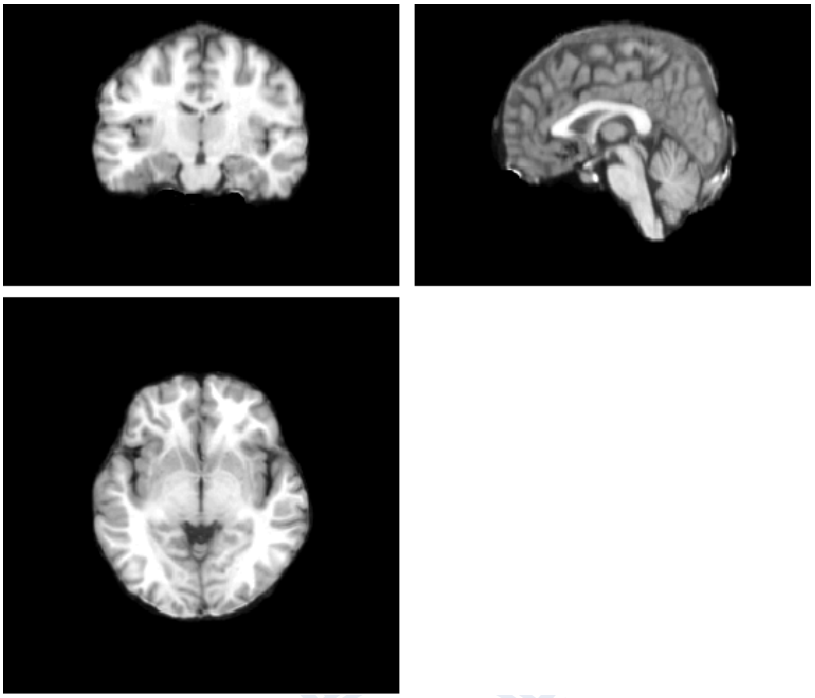

(a)

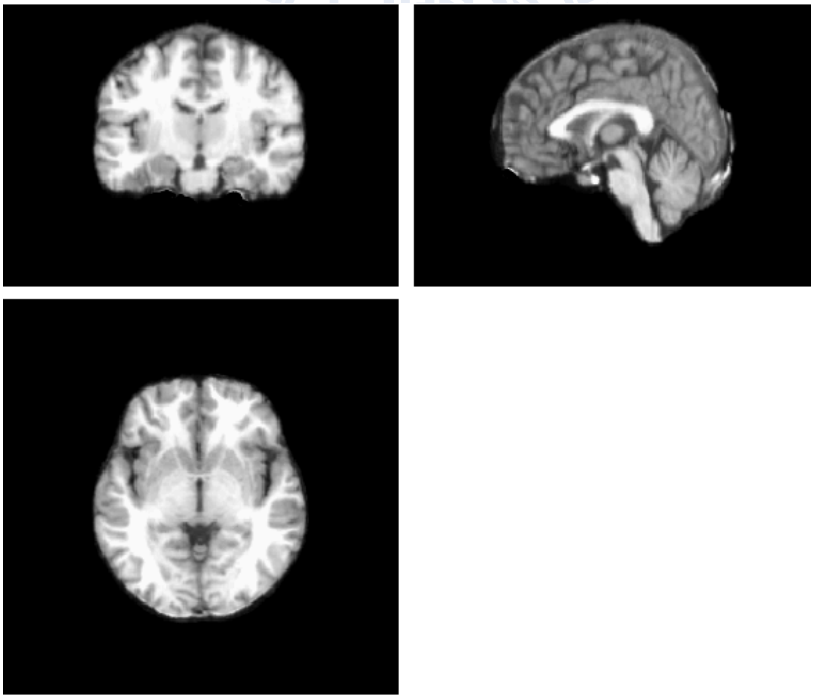

(b)

Figure 4.2: **The representative image through iterative registration.** (a) From iterative affine registration. (b) From iterative affine registration and iterative non-rigid registration. The figure shows in coronal view, sagittal view, and horizontal view.

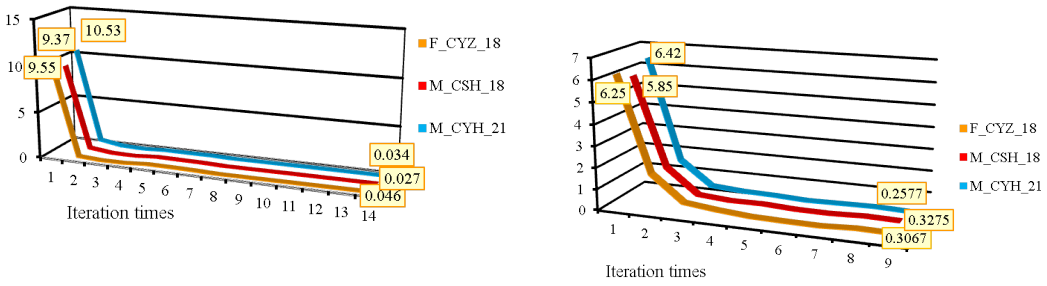

(a) (b)

Figure 4.3: **The convergence of iterative registration.** The criteria of stopping iterative registration based on the intensity of updated representative images for each iteration times. As the intensity variance of the representative image less than 0.05%, the iterative registration would be stopped. This figure shows the convergence of three different initial reference subject images.

4.2.2 Outlier Brain Images

The constructed template should not bias to a specific individual subject which has significant larger transformation than other subject images. Therefore, we define a outlier removing criteria to remove the outlier of subjects. The outlier removing criteria has shown in Chapter 2.3.7. In the construction procedure using a 23 years old male subject as initial (Fig. 4.1) there are six subjects had been seen as outlier subjects. Fig. 4.4 shows the raw image of outlier(left), the outlier image register to the template space (middle) and overlap these two images (right).

4.2.3 Average Brain Template Image

The procedure of constructing brain template will obtain a updated representative image after the iterative affine registration and non-rigid registration. This representative image is also the template space for the input subject group. In order to any analysis or comparison

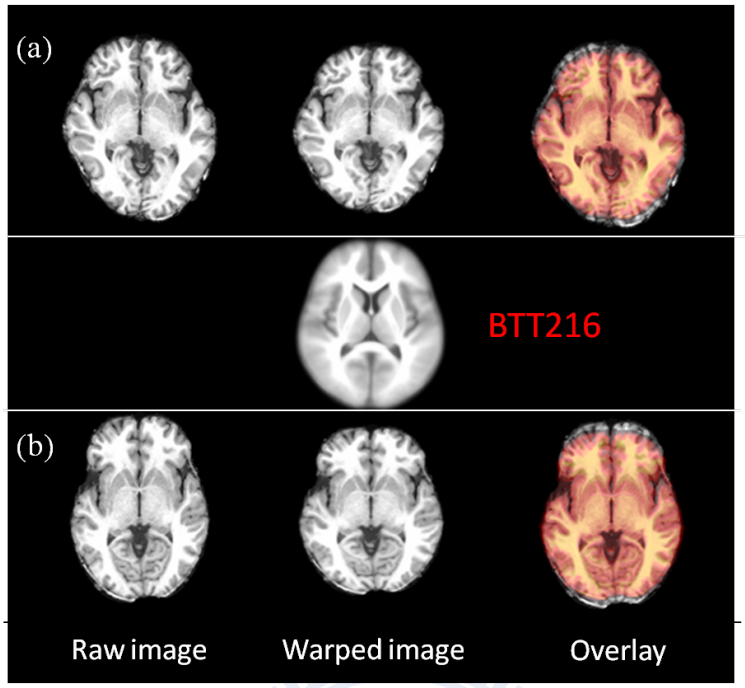

Figure 4.4: **The outlier images.** This figure presents two outlier images from the construction procedure. Left column shows the outlier only for rotation and translation alignment to template space. Middle column shows the scaling and shearing effect from the left column images. The middle image is target image which is our constructed BTT216 template. Right column overlaps the images of middle column onto the images of left column.

between each individual subjects, we will normalize the subject image into this template space. As the representative image is a high contrast image with clear brain structure bias to the initial selected reference image, our target is to obtain a template image with full brain structure information of each subject images. An average template image from the warped subject images which mapped into the representative image should provide more information.

The averaged template image is obtained by averaging all subject images do registration into the template space. The result of the warped image is shown in Fig. 4.5. Fig. 4.5(a) shows the average template image only through the iterative affine registration. Fig. 4.5(b) shows the average template image through the affine and non-rigid registration where the template space was created through the whole iterative affine an non-rigid registration.

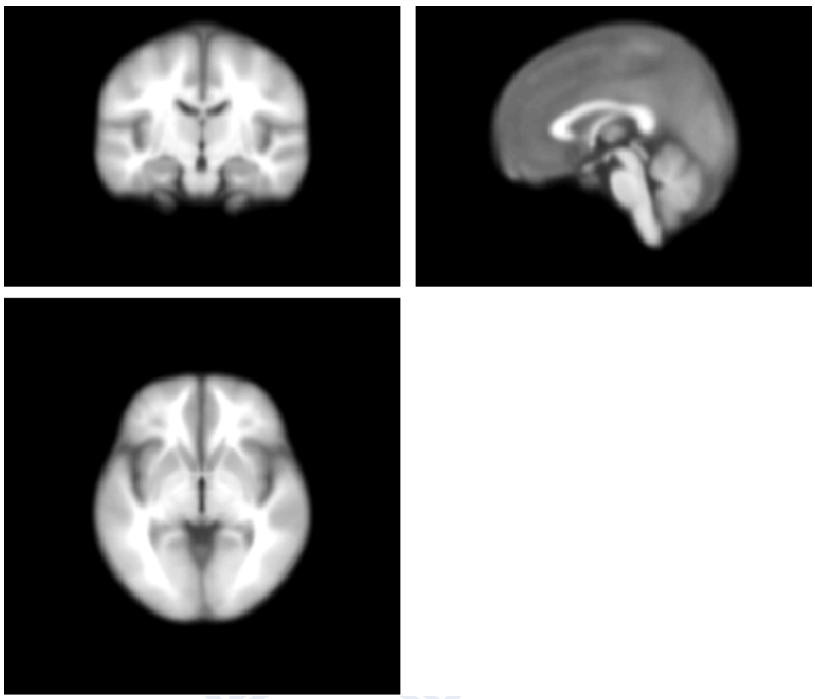

(a)

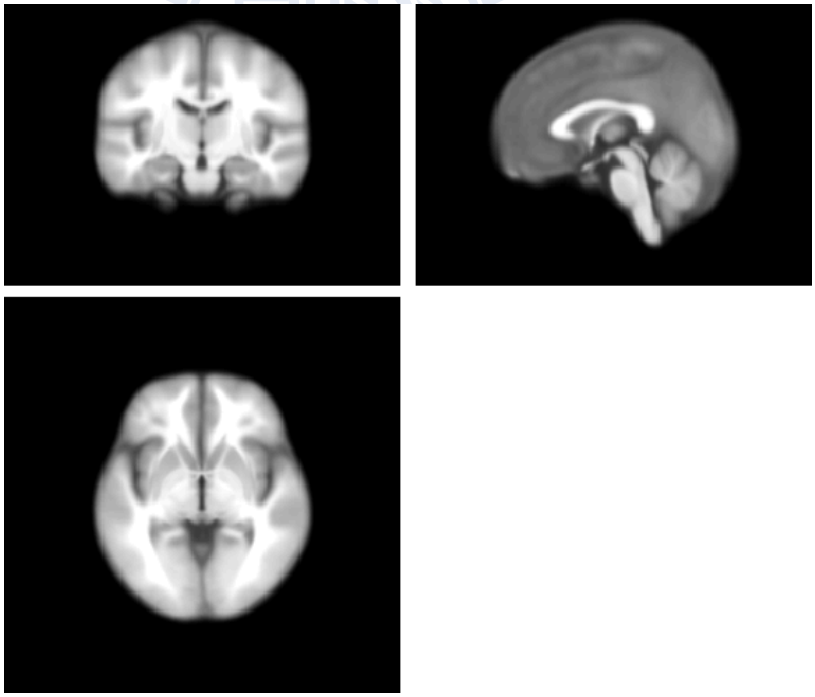

(b)

Figure 4.5: **The average template through iterative registration.** (a) From iterative affine registration. (b) From iterative affine registration and iterative non-rigid registration. The figure shows in coronal view, sagittal view, and horizontal view.

4.2.4 Brain Tissue Template Image

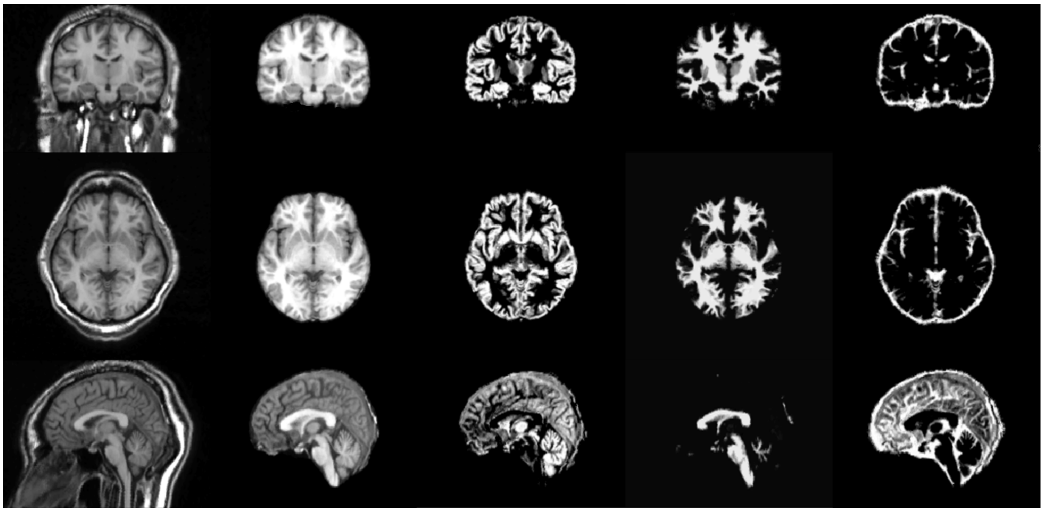

(a)

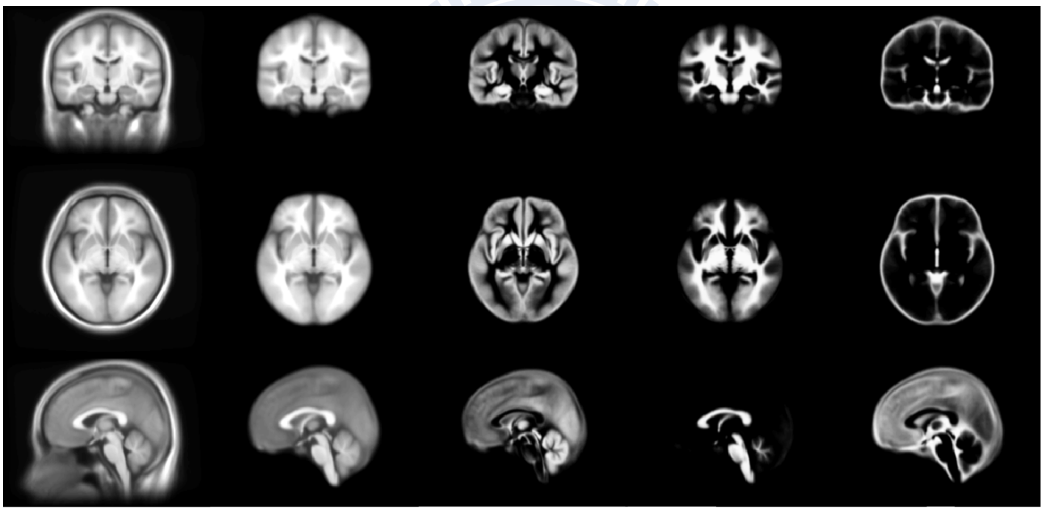

(b)

Figure 4.6: **The different kinds of brain tissue template space and image.** (a) The brain-only, whole-brain and brain tissue representative image (template space). (b) The brain-only, whole-brain, and brain tissue average template image. Each subfigure shows in coronal view, horizontal view, and sagittal view (from up to down). From left to right are brain-only, whole-brain, grey matter, white matter, and cerebrospinal fluid images.

From the steps of tissue segmentation, we will obtain the the whole-brain, brain-only and brain tissue images. The construction procedure apply on brain-only image to obtain the brain-only representative image and averaged template image (Fig. 4.2(b) and Fig. 4.5(b)). We also apply the same transformation on the whole-brain, grey matter, white matter and cerebrospinal fluid images. Fig. 4.6 shows the representative images and averaged template images which are the average warped images in the template space. We named these constructed brain template in Taiwan based on 216 normal subjects were BTT216.

4.2.5 Study Specific Brain Template Image

The construction procedure could be based on any study-specific data to create the customized template space and image. In this study, we construct the template based on different gender groups and age groups.

Gender Template

The male template is constructed by 86 males with age 32.465±11.872 and the female template is constructed by 130 males with age 36.500±13.086. The initial reference image used the constructed template from the whole subject images in the previous study. The procedure of male template construction removes only one outlier image and two outliers from the procedure constructing of female template. The result template image show in Fig. 4.7(a) and 4.7(a).

Age Group Template

Another customized template constructed based on different levels of age. We divided the subject group into six subgroups per 10-age. The constructed template images are shown in Fig. 4.8.

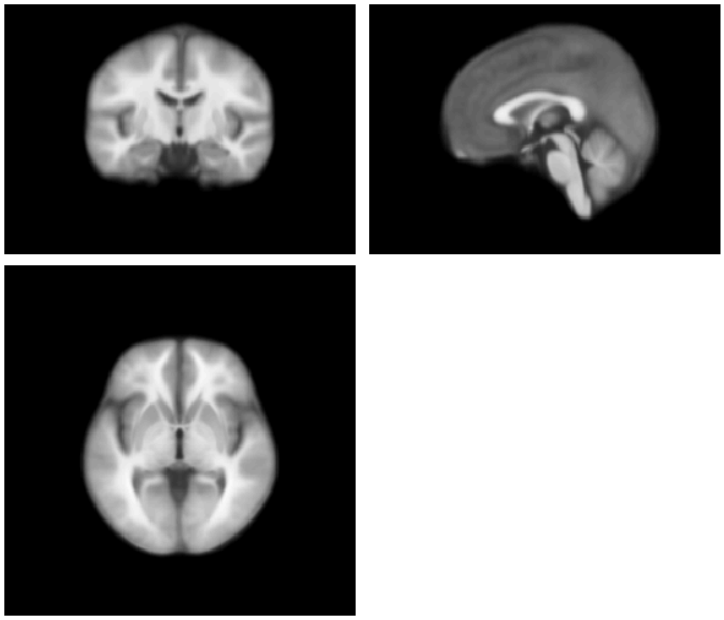

(a)

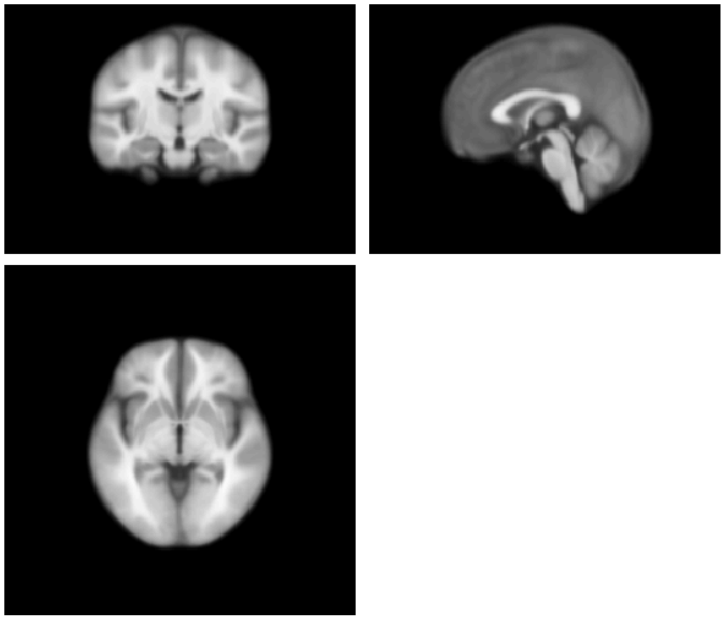

(b)

Figure 4.7: **The customized template based on gender group.** (a) **Male template image.** (b) **Female template image.** Each subfigure shows in coronal view (upper left), horizontal view (lower left), and sagittal view (upper right).

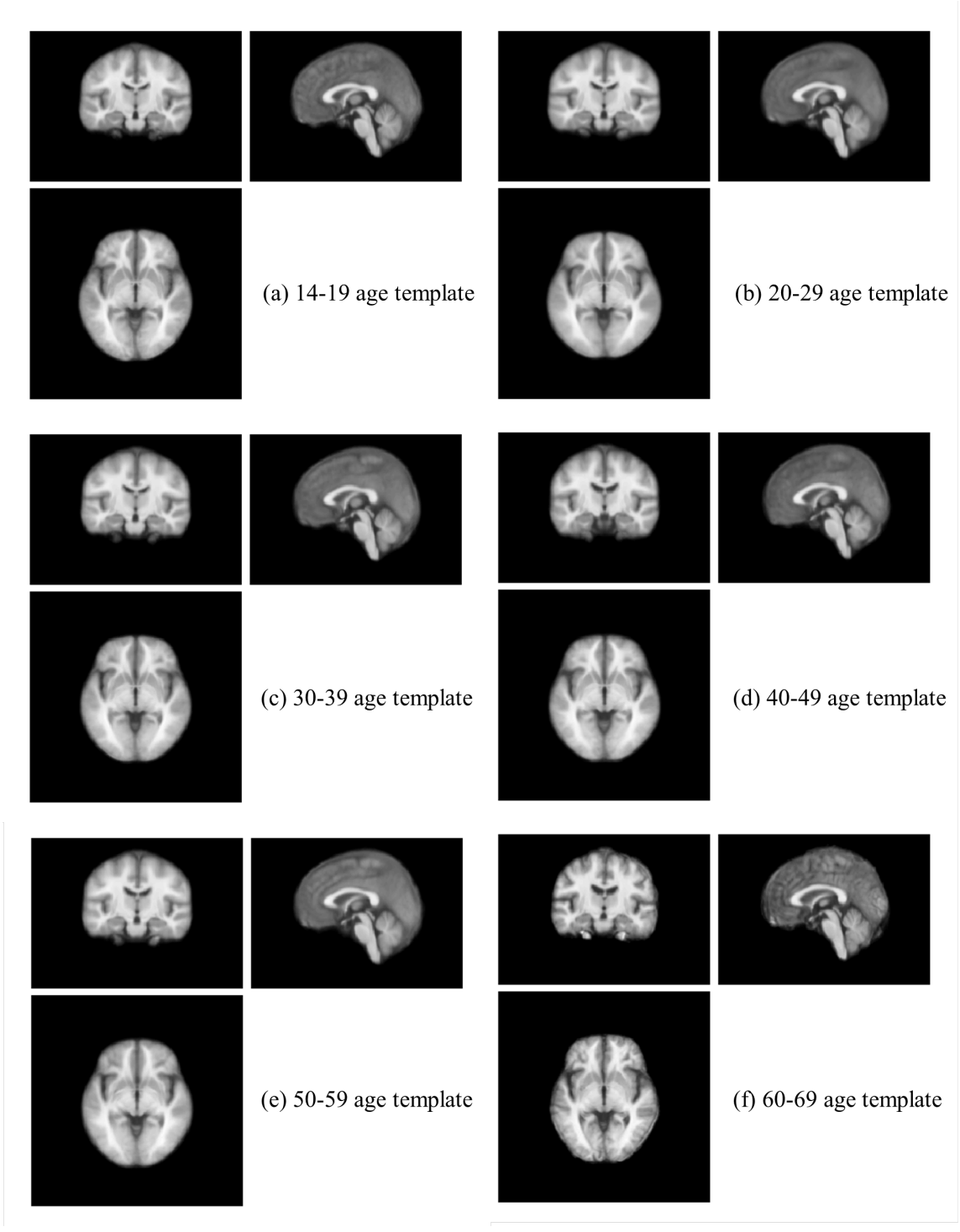

Figure 4.8: **The customized template based on age group.** Divided the subject group into six subguoups by the age of each subjects. The number of each subject groups is shown in Table 4.1.

4.3 Evaluations of Brain Templates

4.3.1 BTT216 template v.s. ICBM152 template

Intensity standard deviation

In this evaluation method, we compute standard deviation of intensity at voxel coordinate in template space for all subject mapping to template space. Fig. 4.9 displays the intensity standard deviation of each voxel from all warped image in different stages of template. The figure also shows the effect from affine to non-rigid and the refinement of iterative registration. The same evaluation method displayed in Fig. 4.10. The variation for each locations of warped image seem larger than BTT216 significantly.

Intensity correlation

Correlation value presents the similarity of two images based on information of image intensity. The value of correlation lies between zero and one. As the correlation value is closer to one, the two images have high similarity. The following figures show the similarity between the template image and the subject images warped into the template space. The comparison template image including the template only constructed from iterative affine registration, the template constructed from whole procedure with iterative affine and non-rigid registration and the well-known ICBM152 template. If the template image is well representing the subject group, the correlation value should be higher. Table 4.3 shows the average correlation value comparing with different template image. In addition to the comparison between BTT216 template and ICBM152 template, we also evaluate the Average191 template which was constructed from 191 normal subject images by Chang [6].

	Template Space			
	Affine Template	BTT216 template	ICBM152 template	Average191
Correlation	0.9694	0.9737	0.9396	0.9581

Table 4.3: **Average correlation between the warped subject images in different template spaces.**

Magnitude and Variance of Deformation Field

Non-rigid registration procedure will obtains 3-dimension deformation field. Table 4.4 shows the average deformation magnitude and standard deviation in each direction and in 3D Euclidean space. ICBM152 template has larger average deformation magnitude than our template. The lower standard deviation also shows the smaller variation of warped image mapping into our template space than ICBM152 template. Fig. 4.11 displays the standard deviation of deformation field for the same voxel of warped images. More transformation may causes more bias in registration. Our template provide a more precise template.

	Reference Template	
	Our Template	ICBM152 Template
Average magnitude	X : 0.3005 ± 0.1854	X : 0.9019 ± 0.6702
Mean$\pm$Std.	Y : 0.5359 ± 0.3789	Y : 1.1703 ± 0.6468
	Z : 0.3980 ± 0.2773	Z : 0.8230 ± 0.4787
	3D : 1.0221 ± 0.5743	3D : 1.7755 ± 0.6557

Table 4.4: **Average deformation magnitude.**

Table 4.5 shows the variation of the magnitude of deformation field based on six labelled landmark. The results show that our constructed template have lower variation than ICBM152 template. It shows the same conclusion in the average deformation magnitude.

Tissue Name	Variance of BTT216	Variance of ICBM152
Anterior commissure (AC)	0.0138	0.1016
Posterior commissure (PC)	0.0041	0.0379
Genu (GU)	0.0719	0.2307
Thalamus (TH)	0.0068	0.0190
Splenium (SP)	0.0106	0.0087
Cerebellar (CB)	0.0342	0.1302

Table 4.5: **Variance of the magnitude of deformation field obtained by normalized into different template images.**

4.3.2 Bisexual template v.s. Gender template

In order to the difference of study-specific subject images, we also constructed the study specific template image. The difference of human brain structure between different gender had already known. We seek to compare the influence of gender template as the template space for specific study.

Table 4.6 shows the averaged correlation of warped images which transformed the subject images into different reference template image. The result shows that gender template is more suitable than bisexual template with higher image similarity in template space. Table 4.7 displays the average magnitude of deformation field obtained from non-rigid registration which transform into different reference template images. Large distortion could reduce the accuracy of image registration. In male template, the average transform magnitude is lower than register into the bisexual template space. But for female subjects, bisexual template seems to provide better coordinate system with smaller average distortion.

	Template		
	Bisexual template	Male template	Female template
Male	0.97166	0.97239	-
Female	0.97503	-	0.97507

Table 4.6: **The average correlation of warped images in bisexual average template and gender templates.**: This table shows the correlation of different gender subject images mapping to their own gender template image and bisexual template image.

4.3.3 Age-Group Template

This section shows the evaluation on the study-specific subject images and aims to the subject group in different ages. Fig. 4.12 shows the average correlation of different age group subjects mapping into different age template. We could find that most subject group divided with different ages had the highest correlation value when mapping to the self constructed template by considering the tendency of each horizontal line which presents different subject groups. We could also find out that each age template image with the highest correlation of warped image from the self constructed subject image group by considering the vertical value from any template image. Only the age group in 20-29 does not perform in highest value.

	Template		
	Bisexual template	Male template	Female template
Male	0.8862	0.8776	-
Female	0.8164	-	0.8742

Table 4.7: **The average magnitude (mm) of deformation field for non-rigid registration to bisexual average template and gender templates.** This table shows the average magnitude of deformation field for different gender subject images mapping to their own gender template image and bisexual template image.

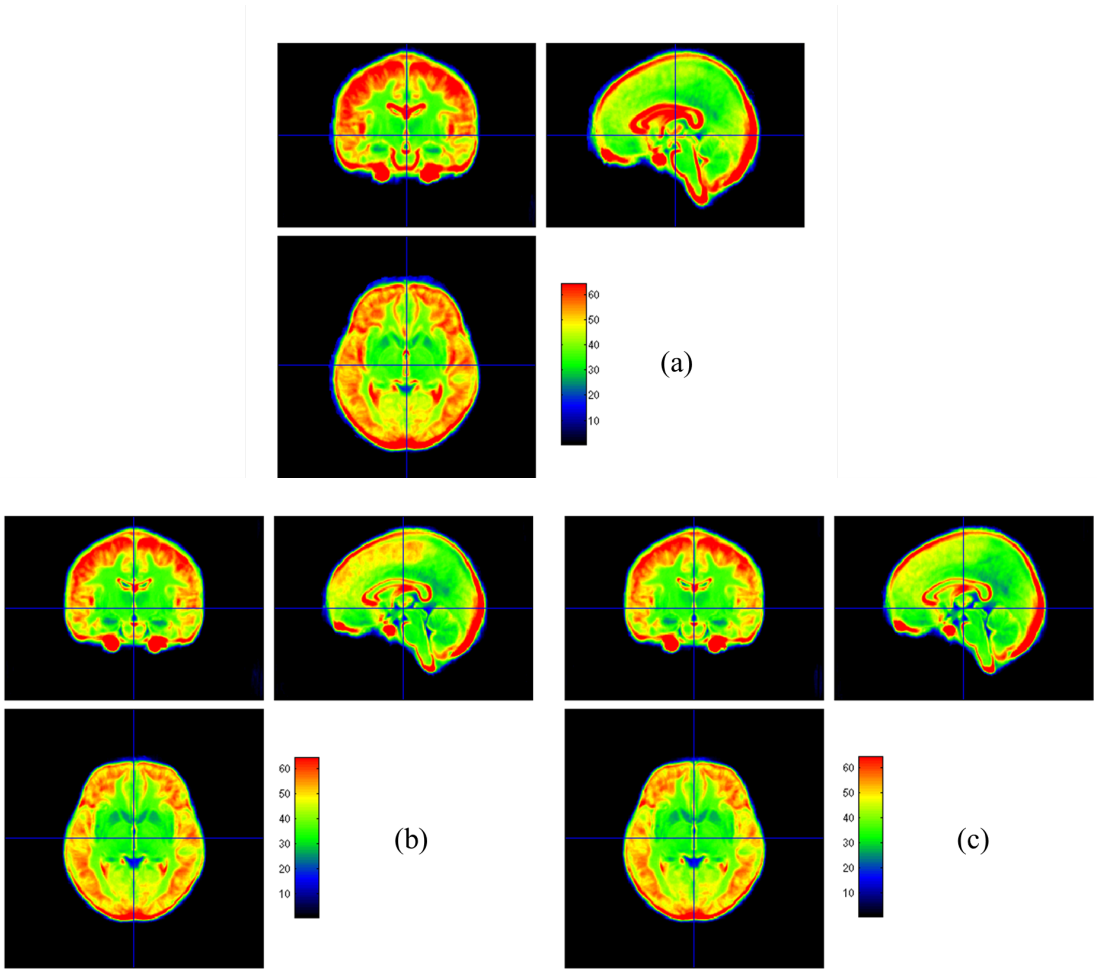

Figure 4.9: **The standard deviation of warped image intensity difference per voxels.** All subject images warp into the template space constructed from (a) 10 times of iteration in **affine registration**. (b) 10 times of iteration in **affine registration** and 1 time of iteration in **non-rigid registration**. (c) 10 times of iteration in **affine registration** and 10 times of iteration in **non-rigid registration**. The range of value is mapped from 0 to 200 into the range of 0 to 64. Each subfigures show in coronal view (upper left), sagittal view (upper right), and horizontal view (lower left).

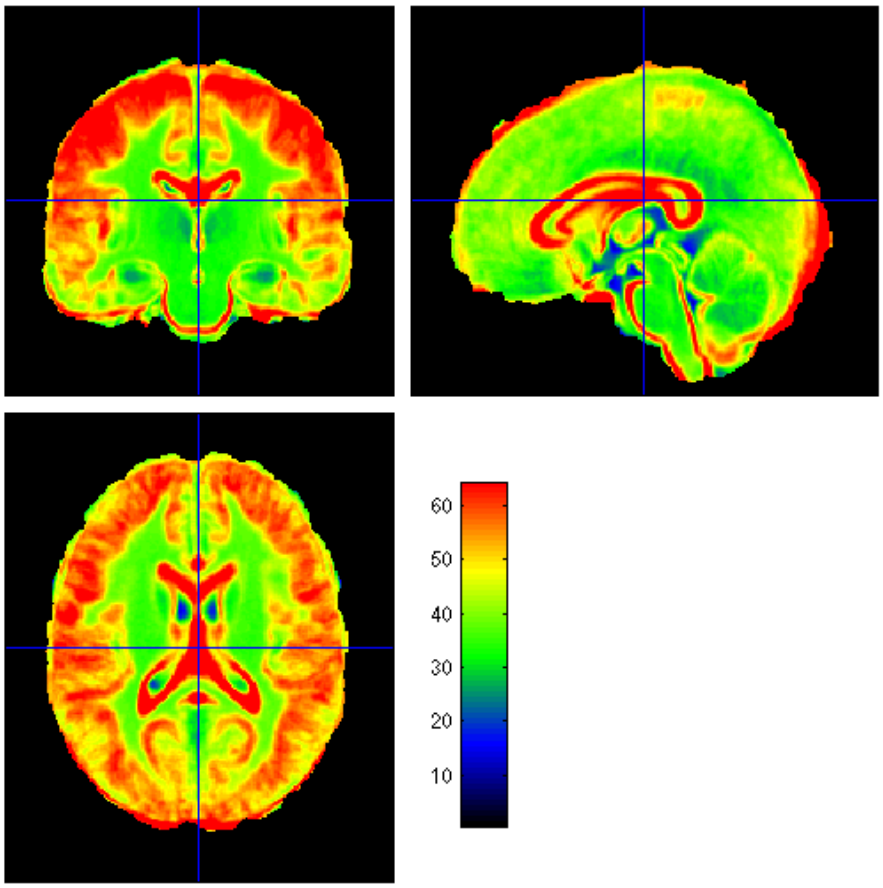

Figure 4.10: **Intensity standard deviation of warped image registered to ICBM152 template.** The range of value is mapped from 0 to 200 into the range of 0 to 64 which represented in colors from black to red.

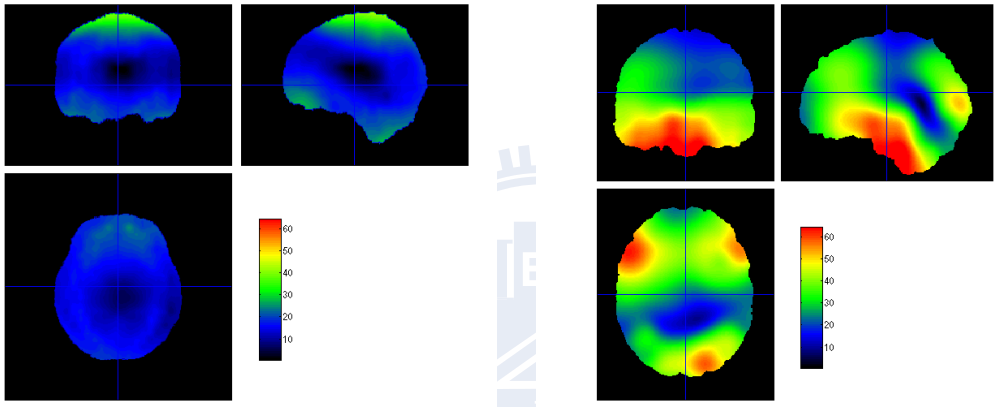

(a) (b)

Figure 4.11: **Standard deviation of deformation field.** This figure shows the evaluation of deformation filed acquired from image registration between subject images and template image. (a) BTT216 template. (b) ICBM152 template. The figure map the value from 0 to 2 into 0 to 64 and the colors mapping from black to red.

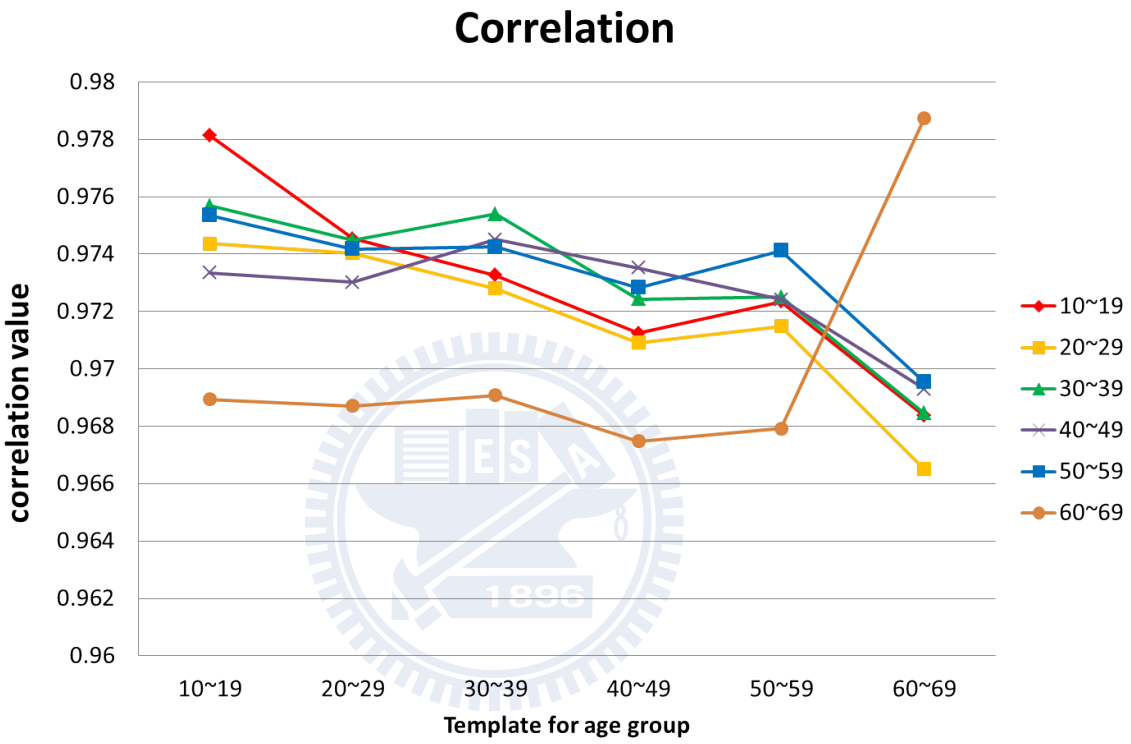

Figure 4.12: **The average correlation of different age group subjects mapping into different age template.** Average correlation calculated from the warped images which transformed into a template image. Six different lines represent different age groups. Vertical axis describe the average correlation value. Horizontal axis represents different template constructed from different age of subject images.

Chapter 5

Discussion

5.1 Comparison between Customized Template and ICBM152

In this section, we compared our template which was constructed from all given 216 subjects in our database with ICBM152 template. From the evaluation method described in Chapter 3, we evaluated the similarity between warped images mapped to the template space which is using image intensity with image correlation and intensity standard deviation. Another evaluation method using deformation field which obtain from image registration with average deformation magnitude and deformation variance and observe the transformation from subject image to template image. In these evaluation experiments, we considered that the customized template constructed from our given subjects is more suitable than ICBM152 template to be the template image for registration.

5.1.1 Correlation between Warped Subject Images

Correlation shows the image similarity based on image intensity. In evaluation method, we warp each individual subject image to the averaged template image space and calculate the average correlation value from those warped images. If the template image could provide better registration accuracy, all warped subject images should have high similarity.

From table 4.3, our constructed customized template with higher correlation than ICBM152 template even only apply iterative affine registration. It shows that the template constructed from our subject images provide better template image for the subject group.

5.1.2 Deformation Field from Individual Brains to Templates

A template space provide a stereotaxic coordinate system for image registration to make all study subject could be aligned in the same coordinate space. Non-rigid registration do the alignment of local brain structure followed by affine registration which apply global shape alignment. The deformation field obtained from the non-rigid registration repre-

sented the transformation of direction and magnitude with the local brain structure alignment for each voxel. The magnitude also represents the variation between template space and individual subject image.

Compared our constructed template with ICBM152 template, table 4.4 shows the magnitude of deformation field in average and standard deviation. The table shows in each direction and the 3D Euclidean space with Euclidean distance in millimeters. The four comparison targets show that customized template has smaller magnitude of deformation than ICBM263 template for image registration. Large deformation may reduce the accuracy of image registration, so our constructed template should provide higher accuracy of image registration than ICBM152 template. Fig. 4.9 displays the average magnitude in 3D Euclidean space for each voxel. Both image adjust into the same intensity range and the value is apply in the color bar from value 0 to 64. Lower value represents in dark color with the meaning of smaller magnitude of deformation. The figure shows obviously that our constructed template image with significant lower average magnitude of deformation field than ICBM152 template at most location. It is more verified that our customized template is better than ICBM152 template.

5.2 The Influence of Initial Selected Reference Image

In our procedure of constructing whole-group template image, we selected an initial reference image from the subject images which has the smallest variation of deformation field from the pairwise non-rigid registration. Our constructing procedure refined the initial reference image into a representative image which also stand for the template space of subject group. In this section, we want to discuss the effectiveness from the selected image.

We randomly selected other two images from the subject group and each image set as the initial reference image in two separate construction procedures following the same procedure we have defined. After we constructed another two template images. We evaluate those two template image and compare with the initial constructed template image. Fig.**??**

shows the result of template image constructed from different initial reference images. The constructed templates seems to be similar from different initial selections. We perform the correlation between these representative image and template image in table 5.1 and 5.2. These tables show in high correlation between these template images and representative images. Therefore, our constructed procedure with iterative registration could reduce the bias condition of different initial reference images.

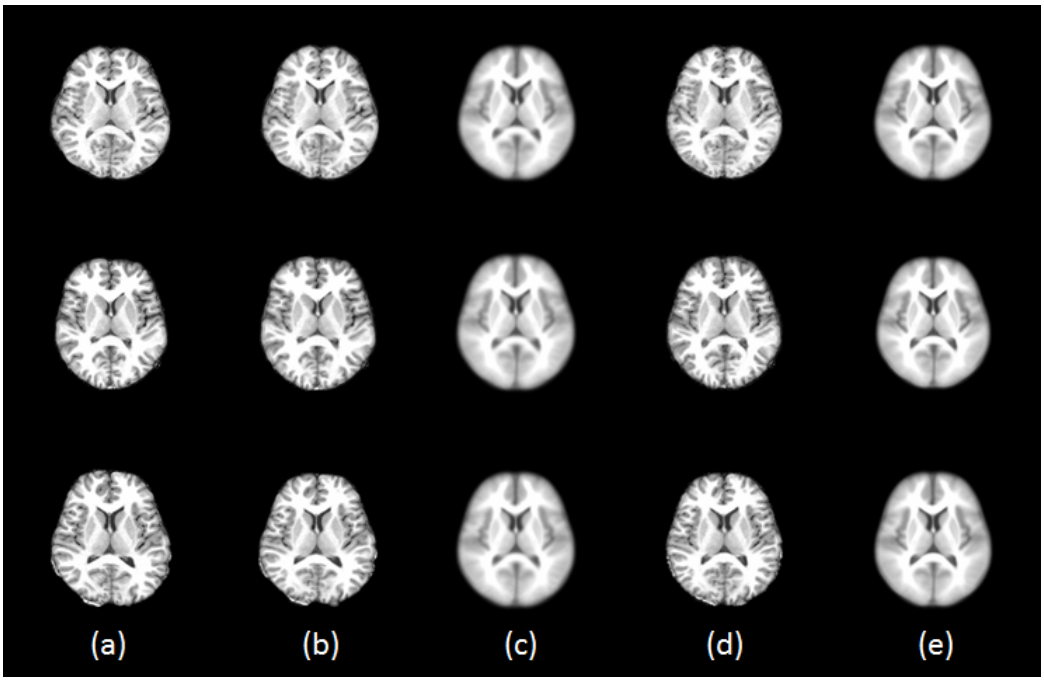

Figure 5.1: **Template constructed from different initial reference images.** This figure shows the representative and template image of three different initial reference images with iterative affine registration and iterative non-rigid registration. (a) Initial reference image. (b) Representative image through iterative affine registration. (c) Template image through iterative affine registration. (d) Representative image through iterative affine registration and iterative non-rigid registration. (e) Template image through iterative affine registration and iterative non-rigid registration.

	Initial reference image		
	F_CJY_23	F_CYZ_18	M_CSH_18
F_CJY_23	1	0.973935	0.957139
F_CYZ_18	-	1	0.951327
M_CSH_18	-	-	1

Table 5.1: **Correlation between representative image of different initial reference.**

	Initial reference image		
	F_CJY_23	F_CYZ_18	M_CSH_18
F_CJY_23	1	0.999421	0.986042
F_CYZ_18	-	1	0.985280
M_CSH_18	-	-	1

Table 5.2: **Correlation between template image of different initial reference.**

5.3 Study Specific Templates

In this section, we evaluated the study specific templates for both gender groups and different age groups. All study specific subject images came from our database with 216 total subjects and the study specific templates would compare to the template constructed from the whole data subject images.

5.3.1 Gender Templates

The gender template construction procedure was applied on the male and female population, 86 males and 130 females. The difference of human brain structure between different gender had already known. We seek to compare the influence of gender template

as the template space for specific study. In evaluation method, we preformed the average correlation in table 4.6 and the average magnitude of deformation field in table 4.7. The results revealed that the gender template is more suitable for the study group.

From table 4.7, the female subject images with smaller average deformation to the bisexual template image than female template image. Deformation field was obtained form the image non-rigid registration which aligned the local structure of brain image. As we obtained the template image from the averaged of all warped image, the local structure may be blur. For image registration, the alignment is based on the contrast of image intensity to align the boundary of different brain tissue. Image with fuzzy condition may affect the registration in disorder. Therefore, we should consider both the value average magnitude of deformation field and the correlation of warped images to evaluate the effect of different template image.

In order to the construction of gender template images to find out the effectiveness between different genders. We also seek to find out more evidence of difference between male and female subjects. Table 5.3 shows the average and standard deviation of total intracranial volume (TIV) of our subject group with 86 males and 130 females. Fig. 5.3 shows the tendency due to different effects of age and gender. It also shows the variation of different brain tissues compare with distinct genders and ages. From the resent study in 2002 [1], the author verified that male brain volume is larger than female brain volume about 10% in cm^3. Our subject group seems to have the same result with the study.

	Brain Volume (cm^3)			
	CSF	GM	WM	TIV
Male	403.545±53.784	687.612±60.467	538.753±47.583	1629.910±126.351
Female	380.565±50.567	619.925±51.499	476.183±35.762	1476.673±107.792

Table 5.3: **Total intracranial volume (TIV) of different gender.**

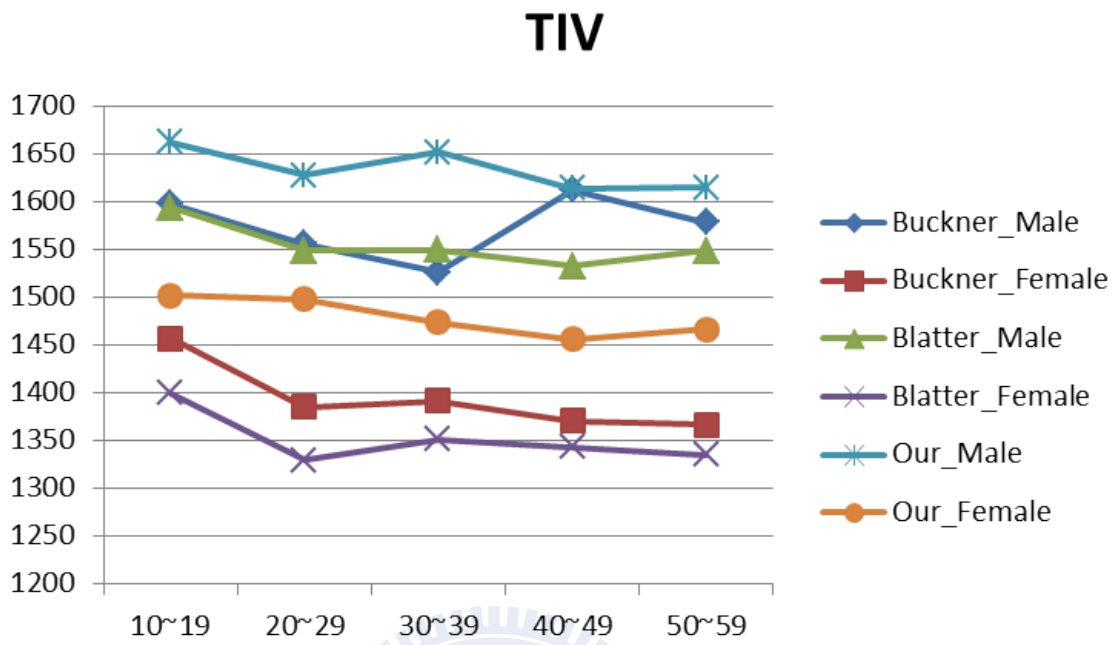

Figure 5.2: **Total intracranial volume (TIV) of gender in different study group.**

5.3.2 Template for Age Group

To construct the age template in different groups, we want to compare the structure difference from human growing. As we want to observe the phenomenon following with age growing, we divide the subjects from database by their ages for 10-year as a boundary. The subject group divide into six subject groups and the data has shown in table 4.1. We construct six age template images based on each age group of subject images. Fig. 4.12 shows that the study-specific template image provide better accuracy of image registration as the warped with higher similarity. The subject numbers from each age group is inconsistent. From the result which shows from Fig. 4.12, the subject group with less study-specific subjects had significant higher correlation when mapping to their own constructed template image, such as age group in 10-19 and 60-69. Due to the template image is constructed by averaged of all warped images. The averaged image with less warped image will bias to those subject images of warped images. This could also shows the importance of study-

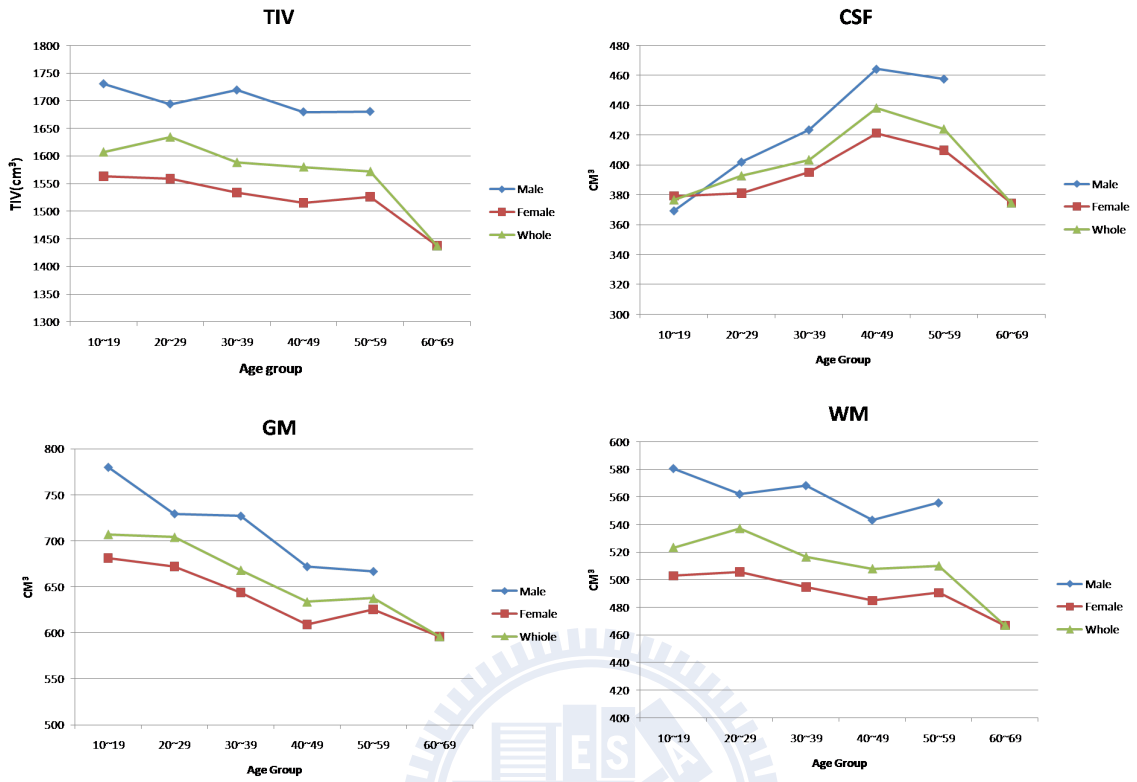

Figure 5.3: **Total intracranial volume (TIV) of different genders and ages.** Upper left shows the tendency of TIV following with distinct genders and ages. Upper right displays the brain volume of cerebrospinal fluid with distinct genders and ages. Lower left shows in grey matter and lower right shows in white matter.

specific template image when the numbers of study subject images are not large enough.

As the same study of the variation between different gender in brain structure, table 5.4 shows TIV in different age group. The numbers of subject in each age group is shown in table 4.1. From the reference study in 1995 [4] and 2004 [5], both study also divide the subject group from 16-year-old for 10 years as the boundary. Fig. 5.2 shows the comparison of these two different studies. The study from D.D. Blatter et al. [4] in 1995 include 194 normal subjects with 105 females and 89 males. The study from R.L. Buckner et al. [5] with 147 healthy subjects and 90 of them are females and 57 are male subjects.

	Age Group				
	10-19	20-29	30-39	40-49	50-59
TIV	1544.748	1570.608	1526.602	1518.713	1510.741
Std.	126.552	140.549	140.549	126.836	138.518

Table 5.4: **Total intracranial volume (TIV) of different age group.** TIV contain the brain volume of grey matter, white matter and cerebrospinal fluid. Table 4.1 shows the subject numbers and average age of each group.

Chapter 6

Conclusions

In this study, we have developed a construction procedure of customized brain template based on study-specific subject images. All construction procedures were depended on the subject images from our data base without using any well-known template images. The constructed brain template BTT216 with five kinds of brain template images, including whole-brain, brain-only, gray matter, white matter, and cerebrospinal fluid images.

The construction procedure has contained the outlier criterion which removes the subject image may cause large deformation in image registration. Consider the magnitude of scaling and shearing as outlier factors from affine registration. If the translation of scaling or shearing from individual subject image to template image is larger than the outlier boundary we have defined, this individual subject image will be considered as outlier image and removed from the construction procedure.

The comparison with well-known brain template, ICBM152, we have obtained better performance in the evaluation method. We have verified the template variation from the warped images by mapped the subject images into different template images. The correlation between the warped images mapped into BTT216 with higher value and the average magnitude of deformation field with lower variation. Besides, we also have constructed the study-specific template image based on different gender group and group of age. The importance of these specific template image have supported from the calculation of total intracranial volume.

Bibliography

[1] John S. Allen, Hanna Damasio, and Thomas J. Grabowski. Normal neuroanatomical variation in the human brain: An MRI-volumetric study. *American Journal of Physical Anthropology*, 118(4):341–358, 2002.

[2] Brian B. Avants, Paul Yushkevich, John Pluta, David Minkoff, Marc Korczykowski, John Detre, and James C. Gee. The optimal template effect in hippocampus studies of diseased populations. *NeuroImage*, 49(3):2457–2466, 2010.

[3] E. H. Aylward, N. J. Minshew, K. Field, B. F. Sparks, and N. Singh. Effects of age on brain volume and head circumference in autism. *Neurology*, 59(2):175–183, 2002.

[4] D. D. Blatter, E. D. Bigler, S. D. Gale, S. C. Johnson, C. V. Anderson, B. M. Burnett, N. Parker, S. Kurth, and S. D. Horn. Quantitative volumetric analysis of brain MR: Normative database spanning 5 decades of life. *American Journal of Neuroradiology*, 16(2):241–251, 1995. Cited By (since 1996): 272 Export Date: 23 July 2011 Source: Scopus CODEN: AAJND PubMed ID: 7726068 Language of Original Document: English Correspondence Address: Blatter, D.D.; Department of Radiology, LDS Hospital, 8th Ave and C St, Salt Lake City, UT 84103, United States.

[5] Randy L. Buckner, Denise Head, Jamie Parker, Anthony F. Fotenos, Daniel Marcus, John C. Morris, and Abraham Z. Snyder. A unified approach for morphometric and functional data analysis in young, old, and demented adults using automated atlas-based head size normalization: reliability and validation against manual measurement of total intracranial volume. *NeuroImage*, 23(2):724–738, 2004.

[6] Yen-Yu Chang. *Automated construction of MRI brain templates in unbiased stereotaxic space*. Master thesis, National Chiao Tung University, 2008.

[7] A. C. Evans, D. L. Collins, S. R. Mills, E. D. Brown, R. L. Kelly, and T. M. Peters. 3D statistical neuroanatomical models from 305 MRI volumes. In *Nuclear Science Symposium and Medical Imaging Conference, 1993., 1993 IEEE Conference Record.*, pages 1813–1817 vol.3, 1993.

[8] Vladimir Fonov, Alan C. Evans, Kelly Botteron, C. Robert Almli, Robert C. McKinstry, and D. Louis Collins. Unbiased average age-appropriate atlases for pediatric studies. *NeuroImage*, 54(1):313–327, 2011.

[9] Catriona D. Good, Ingrid Johnsrude, John Ashburner, Richard N. A. Henson, Karl J. Friston, and Richard S. J. Frackowiak. Cerebral asymmetry and the effects of sex and handedness on brain structure: A voxel-based morphometric analysis of 465 normal adult human brains. *NeuroImage*, 14(3):685–700, 2001.

[10] Colin J. Holmes, Rick Hoge, Louis Collins, Roger Woods, Arthur W. Toga, and Alan C. Evans. Enhancement of MR images using registration for signal averaging. *Journal of Computer Assisted Tomography*, 22(2):324–333, 1998.

[11] Mark Jenkinson and Stephen Smith. A global optimisation method for robust affine registration of brain images. *Medical Image Analysis*, 5(2):143–156, 2001.

[12] Kamran Kazemi, Hamid Abrishami Moghaddam, Reinhard Grebe, Catherine Gondry-Jouet, and Fabrice Wallois. A neonatal atlas template for spatial normalization of whole-brain magnetic resonance images of newborns: Preliminary results. *NeuroImage*, 37(2):463–473, 2007.

[13] Jia-Xiu Liu, Yong-Sheng Chen, and Li-Fen Chen. Fast and accurate registration techniques for affine and nonrigid alignment of mr brain images. *Annals of Biomedical Engineering*, 38(1):138–157, 2009.

[14] John Mazziotta, Arthur Toga, Alan Evans, Peter Fox, Jack Lancaster, Karl Zilles, Roger Woods, Tomas Paus, Gregory Simpson, Bruce Pike, Colin Holmes, Louis

Collins, Paul Thompson, David MacDonald, Marco Iacoboni, Thorsten Schormann, Katrin Amunts, Nicola Palomero-Gallagher, Stefan Geyer, Larry Parsons, Katherine Narr, Noor Kabani, Georges Le Goualher, Dorret Boomsma, Tyrone Cannon, Ryuta Kawashima, and Bernard Mazoyer. A probabilistic atlas and reference system for the human brain: International consortium for brain mapping (ICBM). *Philosophical Transactions of the Royal Society of London. Series B: Biological Sciences*, 356(1412):1293–1322, 2001.

[15] John C. Mazziotta, Arthur W. Toga, Alan Evans, Peter Fox, and Jack Lancaster. A probabilistic atlas of the human brain: Theory and rationale for its development : The international consortium for brain mapping (ICBM). *NeuroImage*, 2(2, Part 1):89–101, 1995.

[16] Declan G. M. Murphy, Charles DeCarli, Andrew R. Mclntosh, Eileen Daly, Marc J. Mentis, Pietro Pietrini, Joanna Szczepanik, Mark B. Schapiro, Cheryl L. Grady, Barry Horwitz, and Stanley I. Rapoport. Sex differences in human brain morphometry and metabolism: An in vivo quantitative magnetic resonance imaging and positron emission tomography study on the effect of aging. *Arch Gen Psychiatry*, 53(7):585–594, 1996.

[17] F. Sgonne, A. M. Dale, E. Busa, M. Glessner, D. Salat, H. K. Hahn, and B. Fischl. A hybrid approach to the skull stripping problem in MRI. *NeuroImage*, 22(3):1060–1075, 2004.

[18] J. G. Sled, A. P. Zijdenbos, and A. C. Evans. A nonparametric method for automatic correction of intensity nonuniformity in MRI data. *Medical Imaging, IEEE Transactions on*, 17(1):87–97, 1998.

[19] Jean Talairach and Pierre Tornoux. *Co-planar stereotaxic atlas of the human brain : 3-dimensional proportional system : an approach to cerebral imaging*. Georg Thieme, Stuttgart, 1988. 2010286519 by Jean Talairach and Pierre Tournoux ; transl. by Mark Rayport.

[20] Roger P. Woods, Scott T. Grafton, John D. G. Watson, Nancy L. Sicotte, and John C. Mazziotta. Automated image registration: II. Intersubject validation of linear and nonlinear models. *Journal of Computer Assisted Tomography*, 22(1):153–165, 1998.

[21] E. L. Wu, Chen Der You, and Chen Jyh-Horng. The construction of a Chinese brain MRI template. In *Noninvasive Functional Source Imaging of the Brain and Heart and the International Conference on Functional Biomedical Imaging, 2007. NFSI-ICFBI 2007. Joint Meeting of the 6th International Symposium on*, pages 262–264, 2007.

[22] Y. Zhang, M. Brady, and S. Smith. Segmentation of brain MR images through a hidden Markov random field model and the expectation-maximization algorithm. *Medical Imaging, IEEE Transactions on*, 20(1):45–57, 2001.

[23] Karl Zilles, Ryuta Kawashima, Andreas Dabringhaus, Hiroshi Fukuda, and Thorsten Schormann. Hemispheric shape of European and Japanese brains: 3-D MRI analysis of intersubject variability, ethnical, and gender differences. *NeuroImage*, 13(2):262–271, 2001.